# PREDICTION OF SHEAR STRENGTH IN HIGHER STRENGTH CONCRETE BEAMS WITH HIGHER WEB REINFORCEMENT

**By**

**Raja Mustensir Javaid**

**(**2006-NUST-MS Ph.D Str-04)

A Thesis submitted in partial fulfillment of
the requirements for the degree of
**Master of Science**

In

**Department of Civil Engineering**

**National Institute of Transportation**

**National University of Sciences and Technology**

**Rawalpindi, Pakistan**

**(2008)**

This is to certify that

thesis entitled

# PREDICTION OF SHEAR STRENGTH IN HIGHER STRENGTH CONCRETE BEAMS WITH HIGHER WEB REINFORCEMENT

**Submitted by**

**Raja Mustensir Javaid**

Has been accepted towards the partial fulfillment

of

the requirements

for

Master of Science in Civil Engineering

_____

**Brigadier (Retired) Dr. Khaliq-ur-Rashid Kayani**

**National Institute of Transportation, Risalpur**

**National University of Sciences and Technology Rawalpindi**

# PREDICTION OF SHEAR STRENGTH IN HIGHER STRENGTH CONCRETE BEAMS WITH HIGHER WEB REINFORCEMENT

**By**

**Raja Mustensir Javaid**

A Thesis

of

Master of Science

Submitted to the

**National Institute of Transportation**

**Risalpur**

**National University of Sciences and Technology**

**Rawalpindi**

In partial fulfillment of the requirements

For the degree of

Master of Science in Civil Engineering

2008

**DEDICATED**

**TO**

**MY MOTHER, SISTER, WIFE AND DAUGHTER**

# ACKNOWLEDGEMENT

I bow my head in all my humility before Almighty Allah whose blessing have enabled me to complete this undertaking. During the course of my research work, I express my gratitude and heartfelt thanks to my advisor Brigadier (Retired) Khaiq-ur-Rashid Kayani whose constant guidance went a long way in facilitating timely completion of this research.

I extend warm and best wishes to NHA and MCE Concrete Laboratory Staff, without the financial and technical assistance of whom it would not have been possible to carry out most of the experimental work. I am also thankful to the administration of the National Institute of Transportation for their help extended in the research work.

Heartfelt thanks are due to my wife, mother, sister and brothers for their moral support, help and dare say this research work would not have been completed without their prayers and whole hearted encouragement. Throughout my professional carrier, I was fortunate to have the prayers of my father protecting and helping me. He has left this mortal world for his heavenly abode but his prayers were and are even today a source of strength and inspiration for me. I dedicate this work to his memory.

# ABSTRACT

Recent development in concrete technology, especially during the last decade, has made it possible to produce the Higher Strength Concrete on commercial scale. The advantages of using higher strength concrete are numerous as it can economize variety of construction works such as long span bridges, off-shore structures and high rise building. The concrete mixture contains high cement contents, low water cement ratio, high quality aggregates and some admixtures (Super plasticizer and silica fumes etc). When properly mixed, consolidated and cured, such mixture gives higher strength, durability and excellent performance.

An experimental investigation of the shear strength of higher strength concrete beams with high web reinforcement ratio was conducted. Six beams were designed in accordance with provision of ACI 2005. The beams were proportioned to exhibit high flexural strength and fail in shear. Concrete with compressive strength of 8000 to 10,000 psi was used in these specimens. The quantity of shear reinforcement provided in these beams is more than the minimum required by the ACI 2005. These beams had web reinforcement 6 inch centre-to-centre spacing.

# TABLE OF CONTENTS

# LIST OF FIGURES

# LIST OF TABLES

# LIST OF ABBREVIATION/NOTATIONS

| | |
|---|---|
| NSC | Normal strength concrete |
| $f_c^/$ | Compressive concrete strength |
| $f_y$ | Yield strength of tension reinforcement |
| M | Moment |
| $M_n$ | Nominal moment strength according to ACI code |
| V | Shear force |
| s | Stirrups Spacing |
| ρ | Reinforcement ratio (As/bd) |
| b | Beam width |
| d | Effective beam depth |
| h | Overall height of beam |
| Fig | Figure |
| $V_c$ | Shear strength provided by concrete |
| $V_s$ | Shear strength provided by steel |
| a | Shear span |
| $V_n$ | Nominal shear strength |
| $A_s$ | Longitudinal steel area |
| w/c | Water cement ratio |
| Dia | Diameter |
| mm | Millimeter |
| in | Inch |
| psi | Pounds per square inch |

*Chapter 1*

# INTRODUCTION

## 1.1. GENERAL BACKGROUND

It is established that high-strength, ready-mixed concrete utilizing conventional materials can be produced and successfully placed in the field for a multitude of concrete markets. For structural application, high-strength concrete allows a reduction in section thickness and a corresponding reduction in dead load. It expands the creativity and flexibility available to the designer, architect, and engineer and results in economy of design. The 1932 proceedings of the American Concrete Institute (ACI) carried the following introductory paragraph in an article entitled "Advantages in the use of High-Strength Concretes" by Thomas T. Towles: It's probable that there are few subjects to which engineers and designers in this country and abroad are giving more serious consideration than to the possibilities in the use of concrete of a strength vary much in excess of the commonly accepted standards of today. The subject is not one of merely speculative interest, but of an immediate practical importance (National Crushed Stone Association 1975).

Towles went on to describe the design and economic advantages to using 28-day, 7000 psi compressive strength concrete over 3000 psi concrete in arch and long span beam constructions. Other benefits such as reduced number and size of columns, reduced dead load, better resistance to weathering action, and more satisfactory appearance were mentioned.

A careful and lengthy analysis was made by Richart on the use of high strength concrete (6000 psi) in building construction. The following is the summary of his findings describing the advantages using higher strength concrete for various structural elements:

| | |
|---|---|
| • Flat slabs | Reduced dead load |
| • Rectangular beams | Reduced section width/thickness |
| • One-way slabs | Reduce section thickness |
| • T-beams | Reduced section width/thickness |
| • Columns | Greatest reduction in cost because of ability to take full advantage of increased compressive strength of concrete, reduce size, and increased usable floor space |
| • Footing | Major saving through reduced size due to lesser dead loads. |

Other side benefits mentioned were greater durability, high resistance to wear and abrasion, and improved workability. The one disadvantage cited was the potential for greater shrinkage due to the increased cement paste content. Richart's analysis contained this caution, "The use of unusually strong concrete should not be attempted where in neither architect nor structural engineer will take responsibility for thorough and adequate inspection (Richart 1936)".

Very early work in 1929 by Gilkey on proportioning of concrete mixes contained data and curves for estimating w/c ratio, cement contents, and pounds of water for 28 day compressive strength up to 9000 psi. This study also stressed the potential for strength variation by explaining that the same w/c ratio for different cements, aggregates, temperatures of curing, and condition of placing may produce strengths differing by an extremely wide range. Indeed, the need for quality control was recognized by Gilkey when reporting strength levels for "rigid job control" some 500 to 600 psi higher than for "average job control" ( Gilkey 1929 ).

In 1934, high-strength concrete studies revealed that the ultimate strength is dependent mainly upon the integrity and physical properties of the coarse aggregate. The "ability of the coarse aggregate to develop a high degree of bond with the mortar due to the texture of the surface" was also identified as a factor contributing to strength as was "the resistance which pieces of fracture can offer the forces causing failure" (Thoman 1934).

The thickness and quality of the capping material used on concrete test cylinder may have considerably more effect on the compressive strength test results for high-strength than for lower strength concrete (Thaulow 1957). This same research has also shown that paper and cardboard molds have given as much as a 13 percent lower strength than when metal molds were used. Thaulow points to the benefits of good quality control by stating that: "a reduction in the coefficient of variation for the strength test means lower required average strength and a saving in cement cost which will, in many cases, more than pay the expense of better control."

Concrete strength more than 20,000 psi has been used in reinforced concrete structures. Presently design methods, such as those in ACI code, may or may not be applicable to the vastly available higher concrete strength or not. The ACI shear design method uses the truss analogy to predict beam shear strength as the sum of the concrete contribution and the stirrup contribution. In this study truss analogy as well as beam theory is discussed.

## 1.2 ADVANTAGES OF HIGHER STRENGTH CONCRETE

There are several advantages of higher-strength concrete and are summarized as follows:

- In compression, high strength will obviously carry more loads for a given cross section; correspondingly, smaller sections can serve the purpose.
- For flexural members, smaller cross sections are possible. This permits dead load reduction, and in turn longer spans. In economic terms, it can be shown in many cases that high strength concrete saves money.
- For tall concrete buildings, lower-story column are heavily loaded. By use of higher compressive strength, large column section can be reduced.
- Ease of placement and compaction without segregation.
- Higher resistance to freezing and thawing, chemical attack, and significantly improved long term durability and crack propagation.

## 1.3 PHILOSOPHY OF HIGHER STRENGTH CONCRETE MIXTURE

Higher strength concrete mixture are generally characterized by low w/c ratio, high cement content, and presence of admixture types, such as water reducing, set retarding, and mineral admixture like fly ash, ground blast furnace slag, and silica fumes. To make the high strength concrete from locally available material, there are no well defined guide lines similar to the ACI recommended practice for selecting proportions for concrete mixtures. The material and mix proportion are to be selected empirically by extensive laboratory testing. It is an established fact that production of high strength concrete is largely depending on the following factors.

- Comparatively larger amount of cement quantity.
- Lesser w/c ratio.
- Stronger and comparatively smaller sized coarse aggregate.
- Use of suitable high range water reducing concrete admixtures.

## 1.4 SCOPE

The scope of this research is to:

- Provide experimental data to examine the existing empirical expression of ACI code predicting shear capacity of reinforced concrete beams with web reinforcement.
- Suggest measures/methods for better prediction of shear strength of beams.

*Chapter 2*

# SHEAR CHARACTERISTIC OF CONCRETE BEAM

## 2.1 SHEAR IN BEAMS

A beam resists loads primarily by means of internal moments, "M" and shear, "V". In design of the reinforced concrete members, flexure is usually considered first, leading to the section proportions and the arrangements of the reinforcement to provide the necessary moment resistance. Limits are placed on the amount of flexure reinforcement which is used to ensure that if failure were ever to occur; it would develop gradually, giving warning to the occupants. The beam is than proportioned for shear. A shear failure is frequently sudden and brittle; the design for shear must ensure that the shear strength equals or exceeds the flexural strength at all points in the beam. The manner in which shear failure can occur varies widely depending on the dimensions, geometry, loading and properties of the members, Figure 2.1 a & b (Appendix I).

## 2.2 SHEAR BEHAVIOR OF BEAMS WITH WEB REINFORCEMENT

The purpose of providing web reinforcement is to ensure that the full flexural capacity can be developed. Prior to incline cracking, the strain in the stirrups is equal to the corresponding strain of the concrete. Since concrete cracks at a very small strain, the stress in the stirrups prior to the inclined cracking will not exceed 3 to 6 ksi. Thus stirrups do not prevent inclined cracks from forming. They come only into play after the cracks have formed. Prior to flexural cracking, the entire shear is carried by the uncracked concrete. Between flexural and inclined cracking, the external shear is resisted by, $V_{cz}$ (Shear in compression zone), $V_{ay}$ (Vertical component of the shear transferred by aggregates interlock) and $V_d$ (Dowel action). Eventually, the stirrups crossing the crack yield, the inclined crack opens more rapidly. As the inclined crack

widens, $V_{ay}$ decreases further, forcing $V_d$ and $V_{cz}$ to increase at an accelerated rate until either a splitting failure occurs, or the compression zone crushes due to combined shear and compression Figure 2.2 ( Appendix I).

Each of the components of this process except $V_s$ (Shear in stirrups) has a brittle load deflection response. As a result, it is difficult to quantify the contribution of $V_{cz}$ , $V_d$ , $V_{ay}$ . In design these are lumped together as $V_c$ (Shear in concrete), referred to as "the shear carried by the concrete". Thus the nominal shear strength, $V_n$ is assumed to be

$$V_n = V_c + V_s$$

A number of experimental programs for the prediction of shear strength in the high strength concrete beams have been carried out. Important conclusions drawn by them are:

- The ACI Code shear design method for slender beams with stirrups is conservative (Andrew 1987).
- Stirrups carry very little shear prior to incline cracking (Andrew 1987).
- As the amount of stirrups increased, the beams displayed improved ductility and failures were less sudden (Andrew 1987).
- After inclined cracking, the stirrups stress increases at much faster rate in beams with low amount of stirrups (Andrew 1987).
- The concrete shear strength contribution, $V_c$, in beams with stirrups, may be as much as 30% lower than predicted by present ACI code equation. Nilson's results were more favorable for high strength concrete beams with stirrups as compared to beams without stirrups (Nilson 1995).

- The number of inclined cracks increased with increasing amount of web reinforcement, indicating an enhanced redistribution of internal forces in beams.
- The crack surfaces were observed to be much smoother in the higher strength concrete beams probably reducing the contribution of aggregate interlock to the shear strength of such beams.
- Beams without stirrups failed suddenly. These beams had only a single diagonal crack on one end of the beam extending throughout the shear span.
- Both shear and diagonal tension failure occur after yielding of the longitudinal reinforcement (Nilson 1998).
- Low amount of longitudinal reinforcement causes few but wider cracks while comparatively heavily reinforced beams fail with large but narrow cracks (Swamy 1985).
- The truss model analysis indicates that an increase in $f'_c$ would increase the strength of the concrete component of the truss (Johnson 1989).

## 2.3 SHEAR MODELS

### 2.3.1 Truss Analogy

The behavior of beams failing in shear must be expressed in terms of a mechanical/ mathematical model before designers can make use of this knowledge in design. The best model for beams with web reinforcement is the truss model. In 1899 and 1902, respectively, Ritter and Morsch, independently, published paper proposing the truss analogy for the design of reinforced concrete beams for shear. These

procedures provide an excellent conceptual model to show the forces that exist in a cracked concrete beam.

As shown in Figure 2.3 and 2.4 (Appendix I), a beam with inclined cracks develops compressive and tensile forces, C and T, in its top and bottom flanges, vertical tensions in the stirrups and inclined compressive forces in the concrete diagonals between the inclined cracks. An analogous truss replaces this highly indeterminate system of forces.

### 2.3.2 Beam Theory

For an elastic homogenous material behaving in the same manner under tension and compression, the distribution of horizontal shear stresses over the depth of a beam may be calculated from first principles. This distribution of shear stress is parabolic for rectangular beam Figure 2.5 (Appendix I), and expressed as:

$$v = 6V / bd^3 \left\{ \frac{d^2}{4 - y^2} \right\} \qquad 2.1$$

The maximum shear stress will therefore occur at neutral axis and given by

$$v = 3V/2bd$$

It can be shown that the maximum tensile stress due to shear will occur normal to a plane at 45º to the plane of maximum shear stress and numerically equal to the shear stress. Equation 2.1 can not be applied to reinforced concrete beams for the following reasons:

- Reinforced concrete is a combination of two different materials whose strength and stiffness differ significantly and is not a homogenous material.
- Concrete is subject to creep and therefore is not truly elastic.

- Cross sections may be cracked or uncracked. Since the extent of cracking at a specified location along the length of the beam is unpredictable, the actual cross sectional properties on which to base computations of moment of inertia, moment of area, and so forth, cannot be determined.
- Because of cracking, the effective cross section of reinforced concrete members varies along their length. In continuous structures, variation in cross section influences the magnitude of internal forces.

For above reasons a precise analytical evaluation of shear stress intensity is not possible for a reinforced concrete beam. Therefore in reinforced concrete beams maximum diagonal tension due to shear is given by:

$$v = V/bj_d$$

where $j_d$ is the internal lever arm.

ACI code takes the value of $j_d$ = 1, for establishing the order of magnitude of the average shear stress on a cross section. The shear stress is computed by dividing the shear force by $b_w$ d, the effective area of concrete:

$$v = V/b_w d$$

where

$v$ = Shear stress at a section

V = Shear force at the section

$b_w$ = Width of beam

d = Distance between compression surface and centriod of tension steel

### 2.3.3 Modified Compression Field Theory

The research has shown that, in general, the angle of inclination of the concrete compression is not 45º. Equations based on variable angle truss provide a more realistic basis for shear design. In addition, tests of reinforced concrete panels subjected to pure shear improved the understanding of the stress-strain characteristics of diagonally cracked concrete. These stress-strain relationships made it possible to develop an analytical model called the modified compression field theory. This theory proved capable of predicting accurately the response of reinforced concrete. The modified compression field model attempts to capture the essential features of the crack pattern idealized as a series of parallel cracks occurring at angle θ to the longitudinal direction (Mitchell and Collins).

The shear stress that can be transmitted across the crack is function of the crack width (w), aggregate size (a), is given as:

$$v_{ci} = \frac{2.16\sqrt{f_c^{/}}}{0.3 + \left(\frac{24w}{a + 0.63}\right)} \qquad 2.1\text{-a}$$

## 2.4 PROPOSED EMPIRICAL EQUATIONS

### 2.4.1 Theodore Zsutty's Equation

Zsutty used regression analysis to evaluate the empirical constant. The final proposed equation is:

$$V_n = 60\left(f_c^{/}\rho\frac{d}{a}\right)^{1/3} + rf_y \qquad 2.2$$

This equation is applicable to concrete compressive strength mostly varying from 2000 to 6000 psi.

### 2.4.2 Andrew G. Mphonde and Gregory C. Frantz

Based on inclined cracking and ultimate shear capacity, they proposed following equations:

$$V_n = \left(1.51\sqrt{f_c'} + 90\right) + rf_y \qquad 2.3$$

$$V_n = \left(1.51\sqrt{f_c'} + 135\right) + rf_y \qquad 2.4$$

Andrew G.Mphonde and Gregory C.Frantz proposed that the ultimate shear capacity of the beam with stirrups is best predicted by:

$$V_n = \left(1.51\sqrt{f_c'} + 90\right) + 1.6rf_y \qquad 2.5$$

This uses the concrete distribution as the inclined cracking capacity of beam without stirrups.

### 2.4.3 ACI Equation

**2.4.3.1.1** I.M.Viest first suggested the present format of ACI equation. Viest simplified the principal stress equation and suggested that shear strength of reinforced concrete beams may be obtained by using the relationship as follows:

$$V_c = \left[A + B\frac{\rho}{\sqrt{f_c'}}\left(\frac{V_d}{M}\right)\right] bd\sqrt{f_c'}$$

where

$V_c$ = Shear stress causing diagonal cracking at a particular location

b = Width of the member

d = Effective depth of tensile reinforcement

$f_c^{/}$ = Concrete strength

$\rho$ = Tensile steel ratio

A = Dimensional constant

B = Dimensional constant

$\frac{V_d}{M}$ = Shear span

ACI and ASCE constituted committee 420 in 1962 to carry out a statistical study for an equation evaluating the shear strength of reinforced non pre-stressed concrete beams. On the basis of statistical analysis of 440 beams, the following values of A and B are obtained:

A = 1.9

B = 2500

By replacing the values of the dimensionless constants:

$$V_c = \left(1.9\sqrt{f_c^{/}} + 2500\rho\frac{V_u}{M_u}d\right)bd \le 3.5\sqrt{f_c^{/}}bd \qquad 2.6$$

### 2.4.4 Present Design Practices

Most existing design codes assume the shear resistance of a beam to be provided by the sum of the resistance due to:

- The concrete which is considered to be equivalent to the load causing diagonal cracking in a beam without shear reinforcement, referred to as the concrete contribution.
- The shear reinforcement.

The concrete contribution is taken as being equal to the shear force at the commencement of diagonal cracking. The shear strength has been formulated by

different researchers using fitting experimental data and involving the major variables affecting the shear strength such as reinforcement ratio, concrete strength, effective depth and a/d ratio.

#### 2.4.4.1 ACI 318-05

ACI 318-05 equation is based on the assumption that the useful shear strength of a beam without shear reinforcement is exhausted, when inclined cracking start. The ultimate shear strength of beam having shear reinforcement is calculated from the following equation:

$$v_c = \left(1.9\sqrt{f_c^{/}} + 2500\rho\frac{V_u}{M_u}d\right)\text{psi}$$

#### 2.4.4.1.1 Canadian Standard Association Concrete Design Code ( CSA-1994)

- **General Shear Design Method**

  Collin and Mitchell introduced the design procedure which is based on modified compression field theory (MCFT). This method use following equations for prediction of ultimate strength of reinforced concrete beams:

$$v_n = v_s + v_c \qquad 2.7$$

$$v_c = \beta b v d_v \sqrt{f_c^{/}}$$

$$v_s = \frac{Avf_y}{s}dv\cot\theta$$

  Where $\beta$ and $\theta$ are the functions of the strain,'$v$' shear stress and's', crack spacing, and

$$v = \frac{V_n}{b_v d_v}$$

- **Simplified Shear Design Method**

  In 1994 Canadian standard association, shear strength of reinforced concrete beam is calculated by following equation:

$$v_n = 2\sqrt{f_c'} + rf_y \qquad 2.8$$

  where $2\sqrt{f_c'}$ is the concrete contribution.

#### 2.4.4.1.2 New Zealand Code

New Zealand code permits calculating shear strength of reinforcement concrete beams by following method:

$$v_u = (0.07 + 10\rho)\sqrt{f_c'} + rf_y \text{ (SI)} \qquad 2.9$$

OR

$$v_u = (0.85 + 120\rho)\sqrt{f_c'} + rf_y \text{ (FPS)} \qquad 2.10$$

The comparison of the above mentioned equations suggested by different codes of practices, suggests that prediction of concrete shear strength is not final and ambiguities exist in contributions attributed to various parameters, such as $f_c'$, a/d ratio, size and spacing of shear reinforcement.

*Chapter 3*

# EXPERIMENTAL PROGRAM

## 3.1 GENERAL

A brief on the materials used and experimental/testing procedures followed for the research program are summarized in the succeeding paragraphs.

## 3.2 ESTABLISHMENT OF VARIABLES AND CONSTANTS

The concrete constituents used in the course of this research, based on availability of time and literature review were divided in two categories, the variable and constant constituents. W/C ratio and percentage of silica fumes were selected. The following constituents were kept constant (Arshad 2006).

- Use of indigenous construction materials with silica fume.
- Dosages and type of High range water reducing agent.
- Size and grading of coarse aggregate.
- Grading of fine aggregate.
- Size of reinforcement.

## 3.3 MATERIALS

### 3.3.1 Cement

The Type I cement conforming to ASTM C 150 and C 595 was used. Results of the tests carried out to ascertain the properties of cement are presented in Table 3.1 (Appendix II). Variation in the chemical composition and physical properties of the cement affect concrete compressive strength more than variations in any other single material.

### 3.3.2 Fine Aggregate

The required range of fineness modulus was 2.70 to 3.20 (Arshad 2006). Sand from Lawrancepur and Margala pan crush was mixed together to bring the value of fineness modulus to 2.88. Results of the tests conducted for verification of properties of sand are tabulated in Table 3.2 (Appendix II). The gradation of the fine aggregate is tabulated in Table 3.3 (Appendix II), and graphically shown in Figure 3.1 (Appendix II).

### 3.3.3 Coarse Aggregate

Samples from Margala, Kiriana, and Kala Chita range being the well known sites for better quality of aggregates were collected. The laboratory test results for the three aggregate sources are tabulated in Table 3.4 (Appendix II). Comparison of the test results indicate that crushed aggregate from Kiriana hills had best physical properties.

For this research the quantity of coarse aggregate in all mix designs was kept constant. Maximum size for the aggregate was kept as 1/2 inches. For gradation purpose only three sizes were considered i.e. 1/2 inch, 3/8 inch, 3/16 inch. The gradation and sieve analysis was determined in accordance with ASTM C 136-93 and is tabulated in Table 3.5 (Appendix II), and graphically illustrated in Figure 3.2 (Appendix II).

### 3.3.4 Silica Fume (SF)

For the purpose of this research, SF was selected as a Pozzolanic cementitious material. SF produces best high early strength and durable concrete as compared to other pozzolanic materials (ACI 2005). The SF inclusion in the concrete mix increases the water demand and there by reduces the workability. More recently, the availability of high range water reducing agent has opened up new possibilities for the use of SF as part of the cementing material in concrete to produce very high strength

or very high level of durability or both (ACI 2005). The chemical composition of the SF is tabulated in Table 3.6 (Appendix II).

### 3.3.5 High Range Water Reducing Agent

The High Range Water Reducing Agent used in the research, is a modified "polycarboxlate" type agent. The dosage was kept constant throughout the research work as 4 per cent by weight of cementitious materials. The technical data of polycarboxlate is tabulated in Table 3.7 (Appendix II).

### 3.3.6 Mixing Water

Potable water from Nowshera was used for entire experimental work while curing compound was used for curing.

## 3.4 WORKABILITY OF FRESH CONCRETE

The concept of low w/c ratio retards the characteristics of fresh concrete workability to its minimum. By use of High Range Water Reducing Agent the reduction in workability due to low w/c ratios is improved. Slump of 48 mm for 15-25% of SF was selected as constant in mix design ( Arshad 2006 ) as tabulated in Table 3.8 (Appendix II).

## 3.5 WATER TO CEMENTITIOUS MATERIAL ( W/C ) RATIO

An important variable in achieving high strength concrete is the water to cement ratio. The relationship between w/c ratio and compressive strength which has been identified in normal strength concrete has been found to be valid for HSC as well. The use of chemical admixtures and other cementations materials have been proven generally essential for producing workable concrete with low w/c ratio. W/C ratio for HSC typically ranges from 0.20 to 0.5 (ACI 2005).

Mix was planned with low w/c ratio ranging from 0.22 to 0.23. Due to very low w/c ratio, workability problems were anticipated therefore polycarboxlate was used accordingly.

### 3.6 MIXING

The mixing of HSC ingredients is little different from normal strength concrete mixing. The concrete containing SF requires very careful and calculated mixing of ingredients. Over mixing of such concrete may produce adverse effect on strength development of the concrete. While preparing concrete in the laboratory, the key is batching the SF at the appropriate time and mixing the concrete adequately. ASTM C 192, Standard Practice for Making and Curing concrete Test Specimens in the laboratory, recommends: "Mix the concrete, after all the ingredients are in the mixer, for 3 minutes, followed by a 3 minutes rest, followed by a 2 minutes final mixing". These recommended mixing times were found not enough to break down the agglomerations and to disperse the SF.

Therefore, the following procedure was adopted to mix the ingredients to attain the full dispersion of admixtures in the mix (Holland 2005):

- SF must always be added with the coarse aggregate and some of the water. Batching SF alone or first can result in head packing or balling in the mixer. Mix SF, coarse aggregates, and water for 0.5 minutes.
- Add the Portland cement and any other cementitious material if any. Mix for an additional 1.5 minutes.
- Add the fine aggregates and use the remaining water to wash in chemical admixtures added at the end of the batching sequence. Mix for 5 minutes, rest for 3 minutes, and mix for 5 minutes. If there are doubts that full dispersion and efficient mixing has not been

accomplished, mix longer. However, SF concrete cannot be over mixed.

## 3.7 CASTING OF SPECIMEN

Casting of specimens was carried out as per ASTM C 192M – 02. Six beams were prepared along with 6 cylinders for each beam with detail in Table 3.9 to Table 3.14 (Appendix II).

### 3.7.1 Description of Specimens

The size and details of the specimens were decided in such a way that they should not fail in flexure. The section selected was 7 ½ x 10 inches with two # 8 bars and two # 4 bars bundled together as shown in Figure 3.3 (Appendix II). The overall depth was kept as 10 inches and effective depth'd' was kept as 8.25 inches. A total of six beams were cast and tested. The beams were designated as BS6-1, BS6-2, and BS6-3. The alphabet B indicates "Beam" and S means spacing between stirrups as 6 inches. The last digit means the serial number in the category.

### 3.7.2 Reinforcing Steel

All the longitudinal bars were # 8 & # 4 deformed bars. The web reinforcement used in the beam was # 3 bar hooked by 18 gauge steel wires. The stress-strain diagram of 1 inch bar is shown in Figure 3.4 (Appendix II). The Grade 60 steel was used for longitudinal bars and Grade 40 steel was used for web reinforcement. The tension test data is given in Table 3.15 (Appendix II).

### 3.7.3 Fabrication of Specimens

The specimens were cast in steel shuttering designed for the purpose. The shuttering was prepared in such a manner that it could be dismantled easily. The steel reinforcement cage was bound with 18 gauge steel wire .The cage was placed in the shuttering over the 1-inch spacers and tied up with the bars. The concrete for the

beams was mixed in a rotary mixer hired from local market. The capacity of the mixer was 7 cubic feet. One batch was prepared for one beam and its associated test cylinders. In one batch, 2 bags of cement were used. The standard cylinders cast with beam were 5 to 6 in numbers for each batch. The beams and associated cylinders were covered with Anti sole E-10 and kept under similar environments. The shuttering was removed from beams after 24 hours. During the process of removing shuttering few hairline cracks were observed. The cracks were observed for their depth and extent. It was established that the cracks had not penetrated into the core of the beam and were only surface cracks occurred by shrinkage due to excessive SF.

### 3.7.4 Specimen BS6-1 to BS6-3

Beams were cast on 3 Feb 2008. The web reinforcement was placed at 6 inches centre to centre spacing. Other details of the subject beams are tabulated in Table 3.17 (Appendix II). The detail of the materials used in each of these beams is tabulated in Table 3.18 (Appendix II).

### 3.7.5 Specimen BS6-4 to BS6-6

Beams were cast on 5 April 2008. The web reinforcement was placed at 6 inches centre to centre. Other details of the subject beams are tabulated in Table 3.19 (Appendix II). The detail of the materials used in each of these beams is tabulated in Table 3.20 (Appendix II).

## 3.8 INSTRUMENTATION

Electrical strain gauges were fixed on web and longitudinal reinforcement for recording the strain at different points in shear span as well as in mid span region. All the beams (BS6-1, BS6-2, BS6-3, BS6-4, BS6-5, BS6-6), had one strain gauge fixed at the center and the other in shear span on longitudinal reinforcement, three strain gauges in shear span on web reinforcement of the beams. The electrical strain gauges

of EA-06-240LZ-120/E nomenclature were used to record the strain in the beams. These gauges had 120.0 + 0.3% grid resistance in ohms with gauge factor 2.080 ± 0.5 at 24 $^{0}$C. These gauges are manufactured with self-temperature compensation characteristics to minimize thermal output. The EA series gauges are a general purpose family of constant alloy strain gauges widely used in experimental stress analysis. EA gauges are constructed with a 0.001-inch (0.03-mm) tough, flexible polyamide film backing. Strain gauges were soldered and checked with the help of digital multimeter.

### 3.8.1 Test Set Up

The specimens were transported to Structure Laboratory of University of Engineering and Technology Lahore, where a 50 ton universal testing machine made by Schmadu Tokyo, Japan, is installed. The machine is hydraulically operated and is connected to the computerized data acquisition system as shown in Figure 3.5 (Appendix II). Fifty (50) tons jack was used for the loading of specimens through a steel girder and base plates to create two point load system. The beams were placed on the supports with the help of a gantry crane.

### 3.8.2 Testing Procedure

Beams were divided into two groups, each group consisting of three beams. The beams were planned to be tested with a/d 2.5. The load was applied after centering and aligning the specimens on the testing machine and making all necessary corrections for recording the load, strain and deflection. The computer automatically acquired the strain, load and deflection data. During the application of load, the cracks were observed and marked on the beams.

*Chapter 4*

# EXPERIMENTAL RESULTS

## 4.1 CONCRETE STRENGTH

Six cylinders were cast from each batch of concrete during the casting of the specimens. Six cylinders for BS6-4, BS6-5 and BS6-6 were tested after 14 and 28 days respectively, and the remaining three cylinders were tested on the day of the testing of beams, Table 4.1 to 4.3 (Appendix III). The average compressive strengths of the concrete are tabulated in Table 4.4 (Appendix III).

## 4.2 STRAIN MEASUREMENTS

The strain was measured by using two electrical strain gauges on longitudinal reinforcement and three on web reinforcement.

## 4.3 TEST BEHAVIOR OF SPECIMENS

### 4.3.1 Specimen BS6-1

The beam was loaded on 25 April 2008 with shear span of 21 inches (a/d = 2.54). The reading from strain gauges, load cell and deflections were recorded using data acquisition system. The initial flexural cracks developed at 161 KN load. Increased load widened the flexural cracks and additional cracks appeared between 161 KN to 203 KN loads. Inclined cracks appeared at a load of 161 KN. Beam failed at 397 KN. Load deflection data and plot are given in Table 4.2 and Figure 4.1 (Appendix III), respectively. Load vs strains and plot are shown in Table 4.8 and Figure 4.7 (Appendix III), respectively. The crack pattern of the beam is shown in the Figure 4.13 a & b (Appendix III).

### 4.3.2 Specimen BS6-2

The beam was loaded on 25 April 2008 with a shear span of 32 inches (a/d = 3.8). Initial flexural cracks appeared at a load of 135 KN. Increased load widened the flexural cracks and additional cracks appeared at 140 KN load. After which no cracks appeared. Beam failed at a load of 330 KN. Load deflection data and plots are shown in Table 4.3 and Figure 4.2 (Appendix III). Load strain data and plots are shown in Table 4.9 and Figure 4.8 a, b & c (Appendix III). Cracking pattern is shown in Figure 4.14 a & b (Appendix III).

### 4.3.3 Specimen BS6-3

The beam was loaded on 26 April 2008 with a shear span of 21 inches (a/d = 2.54). Initial 2 to 3 flexural cracks appeared at a load of 125 KN. Inclined cracks appeared at load of 186 KN after which the beam abruptly failed at 308 KN. The same behavior can be seen in Figure 4.15 (Appendix III), along with cracking pattern Figure 4.15 (Appendix III). The load deflection and load strain data are shown in Table 4.4 and 4.10 (Appendix III). The load-deflection and load-strain plots are shown in Figures 4.3, 4.9 a, b & c (Appendix III).

### 4.3.4 Specimen BS6-4

The beam was loaded on 26 April 2008 with a shear span of 21 inches (a/d = 2.54). Flexural cracks appeared at 102 KN. Increased load widened the flexural cracks and additional cracks appeared at 120 KN load. First inclined crack appeared at 186 KN after which more flexural were observed and old cracks also propagated. Inclined cracks kept on appearing along with propagation of few flexural cracks. Beam failed at a load of 397 KN. The cracking pattern is shown in the Figure 4.16 (Appendix III). The load deflection data and load strain data are shown in Table 4.5

and 4.10 (Appendix III). The load deflection and load strain plots are shown in Figures 4.4 and 4.10 a, b & d (Appendix III).

### 4.3.5 Specimen BS6-5

The beam was loaded on 26 April 2008 with a shear span of 21 inches (a/d = 2.54). Flexural cracks appeared at 111 KN load and continued till 160 KN. Inclined cracks occurred at 201 KN load. Flexural cracks started appearing at 190 KN. Inclined cracks widened with increase in load and beam failed at 349 KN. The load-deflection and load-strain data are shown in Table 4.6 and 4.12 (Appendix III). The load-deflection and load-strain plots are shown in Figures 4.5 and 4.11 a, b, c, d & e (Appendix III). The cracking pattern is shown in Figure 4.17 (Appendix III).

### 4.3.6 Specimen BS6-6

The beam was loaded on 27 April 2008 with a shear span of 21 inches (a/d = 2.54). The initial flexural cracks appeared at 111 KN load. Inclined cracks occurred at 210 KN load. By further increasing the load, the beam failed at a load of 397 KN. The load-deflection and load-strain data are shown in Table 4.7 and 4.13 (Appendix III). The load-deflection and load-strain plots are shown in Figures 4.6 and 4.12 a, b & c (Appendix III). The cracking pattern is shown in the Figure 4.18 a & b (Appendix III).

**4.3.7** Behavior of the beams during the tests can be summarized as under:

- Small flexural cracks occurred between 100 KN and 190 KN loads for shear span to depth ratio of 2.5.
- Extension of existing cracks and appearance of new flexural cracks in the shear span spreading from the load application sections towards the

support. The flexural cracks in the shear spans tend to become more inclined.

- Sudden appearance of a wide diagonal shear crack in one of the shear span. In some cases this crack coincided partially with the inclined part of the flexural cracks. The occurrence of the shear crack was accompanied by drop in the load, which was easy to detect on automatic printed data.
- The average crack angle was between $35^{\circ}$ and $45^{\circ}$.
- All beams failed suddenly with large widening of and sliding in one of the inclined cracks.
- Most of the beams failed in shear, except two which failed in compression shear.

*Chapter 5*

# ANALYSIS AND INTERPRETATION OF TEST RESULTS

## 5.1 GENERAL

Test data was analyzed to understand shear behavior of higher strength concrete beams with web reinforcement. Shear strength of a beam varies with $f_c^{/}$, a/d ratio, and amount of longitudinal reinforcement. Available data from literature was also used to draw logical conclusions.

## 5.2 GENERAL BEHAVIOR OF BEAMS

Four beams (BS6-1, BS6-4, BS6-5, & BS6-6) failed in diagonal shear, where as BS6-2 & BS6-3 beams failed in shear compression. Flexural cracks appeared at mid spans during the early stages of loading. These cracks started at the bottom of the beams where flexural stresses are maximum. They appeared at shear loads of 161 KN, 135 KN, 125 KN, 102 KN, 111 KN, and 111 KN in BS6-1, BS6-2, BS6-3, BS6-4, BS6-5, and BS6-6 respectively. As the load increased, the existing cracks widened and new cracks developed in almost the entire length of the beams. Initial vertical flexural cracks in the shear span became inclined as they propagated above the longitudinal reinforcement. The inclined cracks at the ends of the beam are due to combined shear and flexure. These are commonly known as inclined cracks, shear cracks, or diagonal tension cracks. The average crack angle on the shear span was approximately 42.478 degrees. The inclined cracks in a beam with short shear span followed almost the straight line between the rollers at the load and at support. In case of all six beams, the failure was preceded by large deflections due to yielding of the tensile reinforcement and sudden explosive/blast noise.

## 5.3 MECHANICS OF SHEAR RESISTANCE IN CONCRETE

**5.3.1** Extensive studies of shear models led to the conclusion that shear strength of reinforced concrete beams depends on the following factors:

- Shear Strength of concrete section.
- Longitudinal reinforcement.
- Shear reinforcement.

### 5.3.2 Concrete Contribution $(V_c)$

**5.3.2.1.** For members subjected to shear and flexure, ACI 2005 uses following relation to calculate the shear capacity:

$$V_c = 2\sqrt{f_c'}bd \qquad 5.1$$

where

$V_c$ = Shear strength provided by concrete

$b$ = Web width

$d$ = Distance from longitudinal tension reinforcement

$f_c'$ = Specified compressive strength of concrete.

The effect of the square root of the compressive strength of concrete, $\sqrt{f_c'}$ on the cracking and ultimate shear strength of concrete was investigated. ACI building code has adopted the design equation in which $\sqrt{f_c'}$ is essentially the main variable controlling the shear strength of concrete. The simplified ACI equation that predicts the shear strength of reinforced concrete beams without web reinforcement is of the form $2\sqrt{f_c'}$ psi. Figure 5.1& 5.2 (Appendix IV), shows plot of observed shear

strength of beams with $\sqrt{f_c^{'}}$ . It is observed that the use of $\sqrt{f_c^{'}}$ as a sole predictor of $V_c$ is inappropriate. The shear span-to-depth ratio, $a/d$ should be considered as an important variable since it takes into account the length of the beam and its depth. Equation 5.1 is based on standard test data on 6 inch x 18 inch, prisms loaded at third points with a fixed $a/d$ ratio of 1. It is believed that $a/d$ ratio plays an important role in shear behavior of concrete beams as demonstrated in the dissertation, "prediction of shear strength in higher strength concrete beams without web reinforcement "(khursheed 2008). The relationship of concrete shear strength is obviously inverse with shear span-to-depth ratio and directly proportional to concrete strength and can be expressed as under:

$$V_c = \frac{2\sqrt{f_c^{'}}bd}{a/d} \qquad 5.2$$

### 5.3.3. Longitudinal Reinforcement

**5.3.3.1**. Traditional beliefs and studies state that shear strength of a concrete section is influenced by the amount of longitudinal steel in term of their dowel action. It also reduces the width of cracks which may add to the aggregate interlock loss across the diagonal plane formed by the shear cracks. Longitudinal reinforcement provides resistance to applied shear depending upon the stress in longitudinal steel.

### 5.3.4 Web Reinforcement

**5.3.4.1** In case of web reinforcement, web shear stress denoted by $V_w$, is the shear force in the stirrups over a horizontal plane of area 'b x s':

$$V_w = \frac{A_v f_s}{bs}$$

by using

$$f_s = \alpha f_y$$

where the value of $\alpha$ = Ranges between 0 and 1.

The above equation can be written as:

$$V_w = \frac{\alpha A_v f_y}{bs} \qquad 5.3$$

## 5.4 SHEAR STRENGTH

### 5.4.1 General

Shear failures in reinforced concrete members are sudden and catastrophic in nature and should be catered for in the design. Normally, reinforced concrete members are first dimensioned for flexure and then checked for shear. The effect of shear is to induce tensile stresses on inclined planes oriented at approximately 45° to the plane on which the shear stresses act. Failure occurs when these stresses, along with horizontal stresses due to bending, exceed the diagonal tensile strength of the material. The failures occur in an inclined plane due to the combined effect of shear and flexural stresses. However, it is difficult to determine the value of the diagonal tensile stress in a reinforced concrete beam because the distribution of shear and flexural stresses over a cross section is not very certain. Accordingly, shear strength prediction in reinforced concrete members is an empirical solution based on the assumption that a shear failure at the critical section occurs on a vertical plane when the averaged shear stress at that section, $V/bd$ exceeds the member shear strength.

### 5.4.2 Cracking shear strength

The cracking shear strength $V_{cr}/bd$ is defined as the shear strength at the occurrence of the initial diagonal crack. Cracking starts with the development of a few fine vertical flexural cracks at mid span, followed by reduction of bond between reinforcing steel and surrounding concrete in the support region. The diagonal cracks develop at about 1 ½ d to 2 d from the face of support. The cracking shear strength has to be linked with the amount of longitudinal reinforcement and the relationship is directly proportional. The cracking shear strength can be evaluated as:

$$V_{cr} = V_c + V_d + V_w \qquad 5.4$$

where $V_{cr} - V_c = V_d + V_w$

$V_{cr}$ = Cracking shear strength

$V_d$ = Shear due to dowel action of longitudinal reinforcement at cracking

$V_c$ = Concrete shear strength

$V_w$ = Force in shear reinforcement

**5.4.2.1** It is believed that no stresses are induced in shear reinforcement till the formation of inclined cracks. Therefore, it can be assumed that $V_w \cong 0$ since force in transverse reinforcement is almost negligible till formation of cracks.

Accordingly $V_{cr} = V_c + V_d$.

**5.4.2.2** Figure 5.8 (Appendix IV), shows plot of shear attributed to dowel action, $V_{cr} - V_c$ against measure of shear in longitudinal reinforcement which is dependent upon $a/d$ ratio (Khursheed 2008). Basing on regression analysis of the

results, the trend line shows $V_d = 0.3108\frac{A_s f_y}{a/d} + 18.408$ for the experimental results.

A safe and conservative estimate based on available data for dowel action component of shear resistance can be made using following equation, which incidentally concides with data of beams without shear reinforcement(Khursheed 2008) :

$$V_d = 0.125\frac{A_s f_y}{a/d}$$

### 5.4.3 Ultimate shear strength

The ultimate shear strength $v_u/bd$ is defined as the shear strength when failure occurs. The ultimate/failure shear strength is determined by the ability of the concrete to stabilize the first diagonal crack and to post pone further propagation of the crack into the compression zone. The ultimate shear strength can be:

$$V_n = V_c + V_d^{/} + V_w^{/} \qquad 5.5$$

$$V_d^{/} = V_n - V_c - V_w^{/} \qquad 5.6$$

| | | |
|---|---|---|
| $V_d^{/}$ | = | Shear due to dowel action at ultimate load |
| $V_n$ | = | Nominal shear strength or total shear strength ($V_t$) by multiplying the strength reduction factor |
| $V_w^{/}$ | = | Web shear strength at ultimate load |
| $V_c$ | = | Concrete shear strength |

It is almost certain that web reinforcement will yield or almost to yield at failure. Hence $V_w^{/} \approx A_v f_y$. The concrete contribution, as already discussed, is $V_c = \frac{2\sqrt{f_c^{/}}bd}{a/d}$ at ultimate. In order to evaluate the dowel force at ultimate $V_t - V_c - V_w$ is plotted

against $\frac{A_s f_y}{a/d}$. The regression analysis as in Figure 5.6 (Appendix IV), given a trend as $V_d' = 0.6201\frac{A_s f_y}{a/d} - 19.604$ for the experimental results. A safe and conservative estimate based for dowel action component of shear resistance can be made using following:

$$V_d' = 0.4\frac{A_s f_y}{a/d}$$

The nominal shear strength of a reinforced concrete beam with web reinforcement can be estimated as: $V_t = V_c + V_d' + V_w'$

where $V_c = \frac{2\sqrt{f_c'}bd}{a/d}$

$$V_w' = A_v f_{yw}$$

$f_{yw}$ = Yield stress of web reinforcement

$$V_d' = 0.4\frac{A_s f_y}{a/d}$$

## 5.5 SHEAR STRENGTH RELATIONSHIPS

### 5.5.1 Cracking shear strength

From the previous section, an expression for determination of cracking shear force can be proposed as:

$$V_{cr} = \frac{2\sqrt{f_c'}bd + 0.125A_s f_y}{a/d} \qquad 5.7$$

### 5.5.2 Ultimate shear strength

Similarly, the ultimate shear force of a beam can be computed:

$$V_t = \frac{2\sqrt{f_c^{/}}bd + 0.4A_s f_y + A_v f_{yw}}{a/d} \qquad 5.8$$

## 5.6 CONCLUSIONS

- Shear span to depth ratio affects the shear strength of the concrete. More is the ratio, lesser is the strength.
- Shear strength of concrete is directly proportional to the amount of longitudinal as well as the transverse reinforcement present in the beam.
- Shear strength of concrete is directly proportion to its compressive strength.

## 5.7 RECOMMENDATIONS FOR FUTURE WORK

Mechanism of shear resistance is yet to be understood. There is a requirement to carryout extensive studies on the subject before shear in concrete can be understood. Following are the suggested studies:

a. A detailed and well-planned study to account for the shear resistance, provided by longitudinal and transverse steel.

b. Development of shear resistance relationship with cross section development.

c. Effect of a/d ratio on shear strength.

d. Effect of compressive strength $f_c^{/}$, on shear strength to include very high concrete strength.

# APPENDIX I

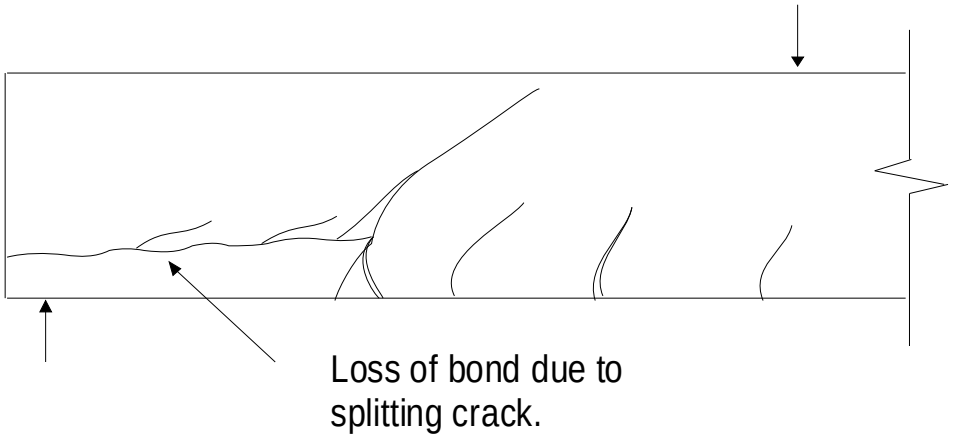


**Fig 2.1a - Shear Tension Failure**

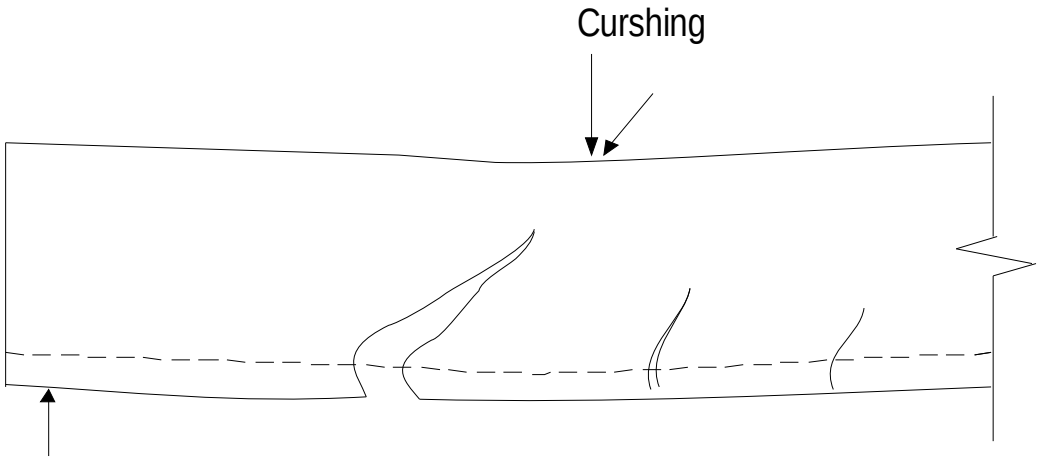


**Fig 2.1b - Shear Compression Failure**

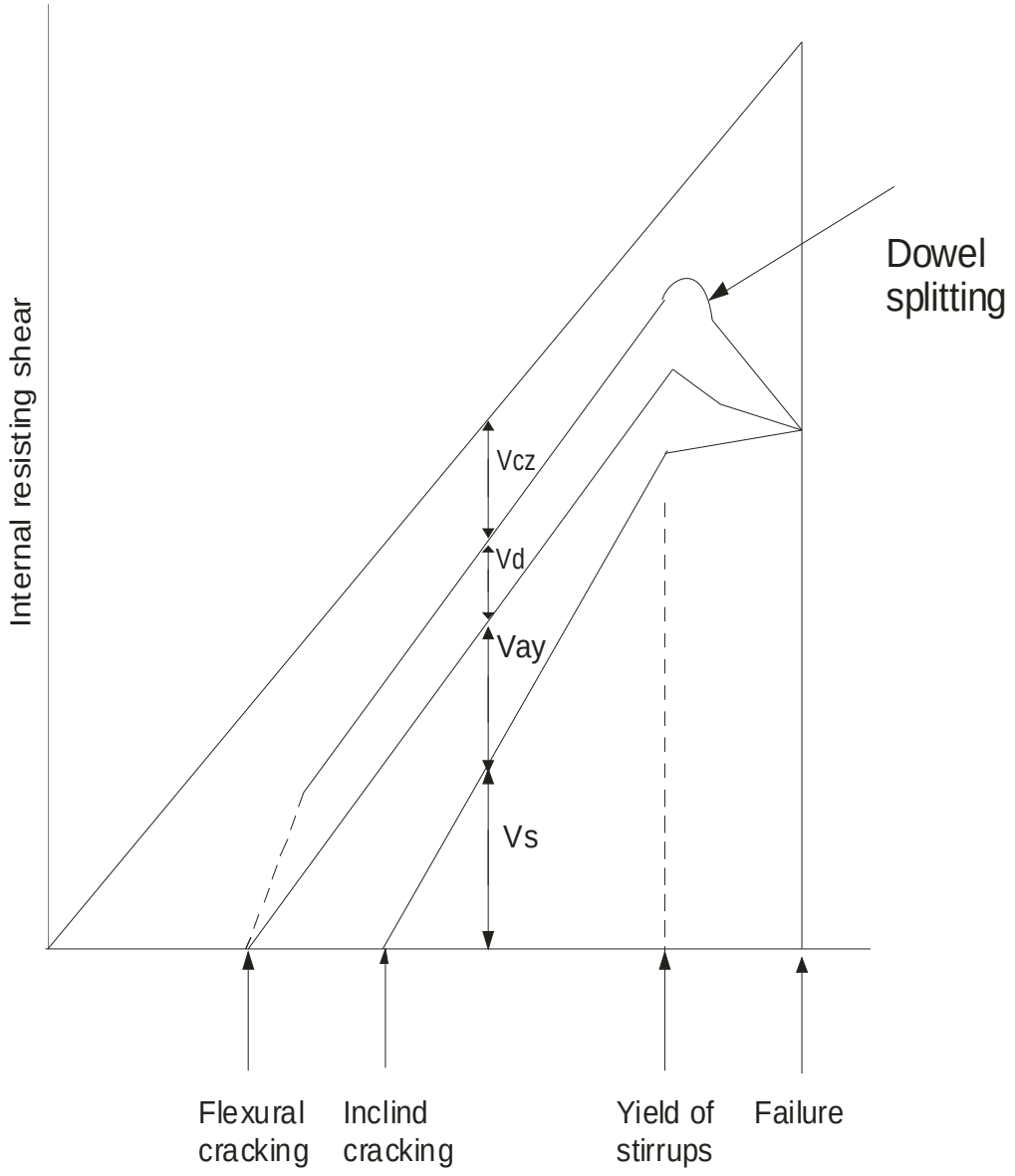


**Fig 2.2 - Distribution of Internal Shear on a Beam**

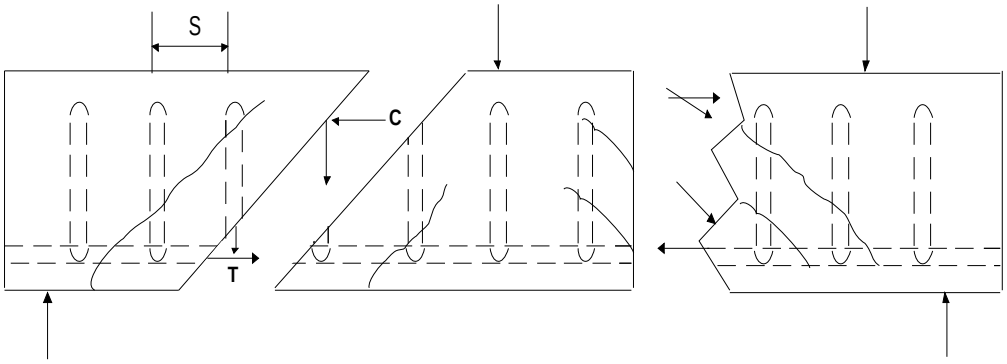


**Fig 2.3 - Internal Forces in a Cracked Beam**

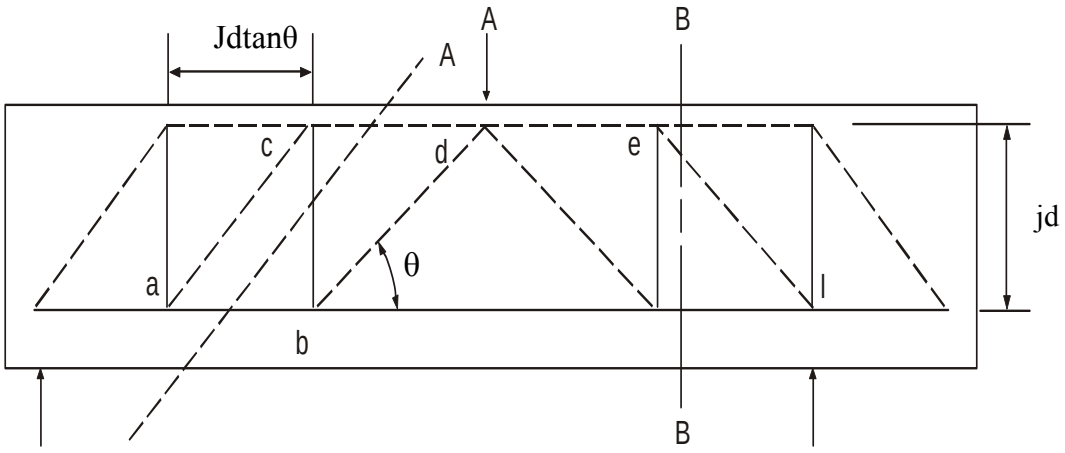


**Fig 2.4 - Pin Jointed Truss**

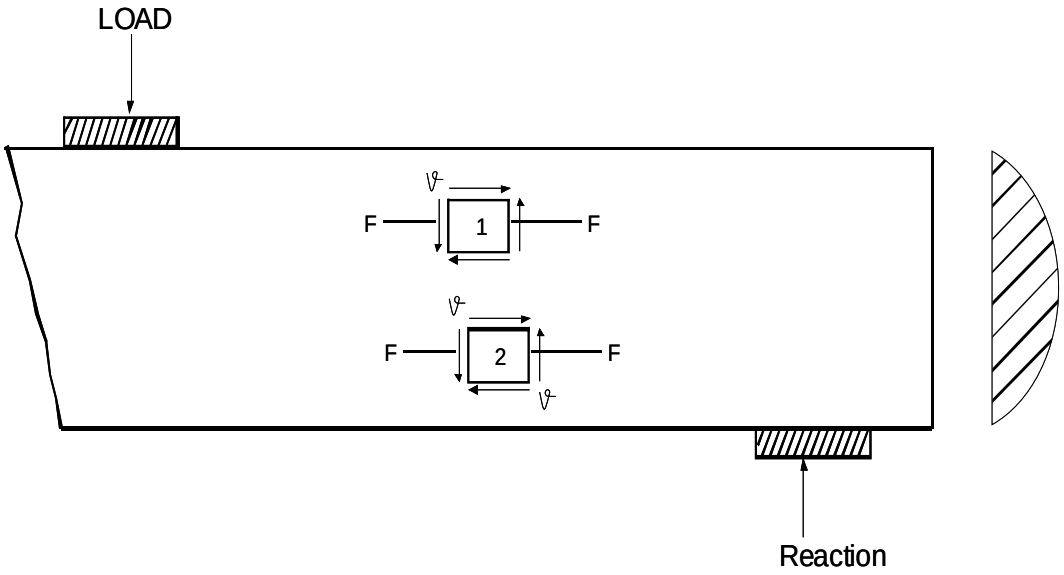


**Fig 2.5 - Flexural and Shear Stresses Acting on Elements in the Shear Span**

# APPENDIX II

Table 3.1 - Properties of Cement

| **Properties of cement** | | |
|---|---|---|
| **Tests** | **Test results** | **Specifications** |
| Specific gravity | 3.10 | ASTM C 188 |
| Initial setting time | 150 minutes at $17^0$C | ASTM C 191 |
| Final setting time | 390 minutes at $17^0$C | ASTM C 191 |

Table 3.2 - Properties of Fine Aggregates

| **Properties of fine aggregates** | | |
|---|---|---|
| **Tests** | **Test results** | **Specifications** |
| Specific gravity | 2.62 | ASTM C 128 |
| Absorption | 0.01 | ASTM C 128 |
| FM | 2.88 | ASTM C 33 |

Table 3.3 - Gradation of Fine Aggregate

| ASTM sieve No | Weight retained (gm) | Percent retained | Cum percent retained | Percent passing | |
|---|---|---|---|---|---|
| | | | | Actual | ASTM C 33 - 93 |
| #4 | 3 | 1 | 1 | 99 | 95-100 |
| #8 | 46 | 9 | 10 | 90 | 80-100 |
| #16 | 129 | 26 | 36 | 64 | 50-85 |
| #30 | 146 | 29 | 65 | 35 | 25-60 |
| #50 | 105 | 21 | 86 | 14 | 10-30 |
| #100 | 43 | 9 | 95 | 5 | 2-10 |
| #200 | 17 | 4 | | | |
| Pan | 7 | 1 | | | |

Table 3.4 - Comparisons of Aggregate Properties

| Sample | Impact value (percent) | Crushing value (percent) | Abrasion value (percent) | Specific gravity |
|---|---|---|---|---|
| Margala | 15.2 | 21.6 | 19.2 | 2.7 |
| Kiriana | 7.9 | 11.58 | 8.9 | 2.91 |
| Kala Chita | 16.2 | 22.5 | 19.2 | 2.81 |

Table 3.5 - Gradation of Coarse Aggregate

| Sieve size (mm) | Percent retained | Cumulative percent retained | Percent passing | |
|---|---|---|---|---|
| | | | Actual | ASTM C 33 - 93 |
| 19 | 0 | 0 | 100 | 100 |
| 12.5 | 10 | 10 | 90 | 90-100 |
| 9.5 | 50 | 60 | 50 | 40-70 |
| 4.75 | 40 | 100 | 0 | 0-15 |

Table 3.6 - Chemical Compositions of SF

| **Chemical composition** | **Percentage** |
|---|---|
| $SiO_2$ | 92 |
| $AI_2O_3$ | 0.6 |
| $Fe_2O_3$ | 1.0 |
| CaO | 0.4 |
| MgO | 1.5 |
| $K_2O$ | 0.8 |
| $Na_2O$ | 0.5 |

Table 3.7 - Technical Data of polycarboxlate

| **Attribute** | **Aqueous solution of modified Polycarboxlate** |
|---|---|
| Appearance | Greenish liquid |
| Density | 1.10 Kg / Liter |
| Ph-value | 6.8 |

Table 3.8 - Workability of Mix

| **Percentage of silica fume** | **Slump values (mm)** |
|---|---|
| | **Using 4 per cent of High Range Water Reducing Agent** |
| 25 | 45 |

Table 3.9 - 28 days compressive strength of cylinders BS 6-1

| **Specimen** | **Size of cylinders (Inches)** | **Compressive strength 28 days** |
|---|---|---|
| BS 6-1/1 | 6x12 | 6900 |
| BS 6-1/2 | “ | 6700 |
| BS 6-1/3 | “ | 6600 |
| BS 6-1/4 | “ | 6500 |
| BS 6-1/5 | “ | 6500 |
| BS 6-1/6 | “ | 6600 |
| Average | - | 6633.33 |

Table 3.10 - 28 days compressive strength of cylinders BS 6-2

| **Specimen** | **Size of cylinders (Inches)** | **Compressive strength 28 days** |
|---|---|---|
| BS 6-2/1 | 6x12 | 7000 |
| BS 6-2/2 | “ | 6800 |
| BS 6-2/3 | “ | 6500 |
| BS 6-2/4 | “ | 6900 |
| BS 6-2/5 | “ | 6300 |
| BS 6-2/6 | “ | 6700 |
| Average | - | 6700 |

Table 3.11 - 28 days compressive strength of cylinders BS 6-3

| **Specimen** | **Size of cylinders (Inches)** | **Compressive strength 28 days** |
|---|---|---|
| BS 6-3/1 | 6x12 | 6850 |
| BS 6-3/2 | “ | 6700 |
| BS 6-3/3 | “ | 6600 |
| BS 6-3/4 | “ | 6900 |
| BS 6-3/5 | “ | 6600 |
| BS 6-3/6 | “ | 6900 |
| Average | - | 6758.33 |

Table 3.12 - 28 days compressive strength of cylinders BS 6-4

| **Specimen** | **Size of cylinders (Inches)** | **Compressive strength** | |
|---|---|---|---|
| | | **14 days** | **28 days** |
| BS 6-4/1 | 6x12 | 8400 | 9800 |
| BS 6-4/2 | “ | 8550 | 8950 |
| BS 6-4/3 | “ | 8650 | 8750 |
| Average | - | 8558.33 | 9300 |

Table 3.13 - 28 days compressive strength of cylinders BS 6-5

| **Specimen** | **Size of cylinders (Inches)** | **Compressive strength** | |
|---|---|---|---|
| | | **14 days** | **28 days** |
| BS 6-5/1 | 6x12 | 8350 | 10000 |
| BS 6-5/2 | “ | 8600 | 9900 |
| BS 6-5/3 | “ | 8400 | 9700 |
| Average | - | 8516 | 9700 |

Table 3.14 - 28 days compressive strength of cylinders BS 6-6

| **Specimen** | **Size of cylinders (Inches)** | **Compressive strength** | |
|---|---|---|---|
| | | **14 days** | **28 days** |
| BS 6-6/1 | 6x12 | 8750 | 10500 |
| BS 6-6/2 | “ | 8800 | 10000 |
| BS 6-6/3 | “ | 8650 | 9950 |
| Average | - | 8683.33 | 9975 |

Table 3.15 - Stress Strain Curve Data (1" Dia Bar)

| Load (tons) | Stress (psi) | Strain |
|---|---|---|
| 0 | 0 | 0 |
| 1 | 3049.479 | 0 |
| 2 | 7280.392 | 0.000137 |
| 3 | 11511.3 | 0.000275 |
| 4 | 15742.22 | 0.000412 |
| 5 | 19973.13 | 0.000549 |
| 6 | 24204.04 | 0.000687 |
| 7 | 28434.95 | 0.000778 |
| 7.5 | 30550.41 | 0.000870 |
| 8.5 | 34781.32 | 0.000916 |
| 9 | 36896.78 | 0.001007 |
| 9.5 | 39012.24 | 0.001053 |
| 10 | 41127.69 | 0.001190 |
| 10.5 | 45358.6 | 0.001282 |
| 11 | 45358.6 | 0.001282 |
| 11.5 | 47474.06 | 0.001328 |
| 12 | 49589.52 | 0.001419 |
| 13 | 53820.43 | 0.001602 |
| 13.5 | 55935.89 | 0.001694 |
| 14 | 58051.34 | 0.001923 |
| 15 | 62282.25 | 0.023256 |
| 18 | 74947.99 | 0.046512 |
| 21 | 87667.73 | 0.093023 |
| 24 | 100360.5 | 0.162791 |
| 24.5 | 102475.9 | 0.209302 |
| 19.8 | 82590.63 | 0511628 |

Table 3.16 - Stress Strain Data (3.8" Dia Bar)

| Load (tons) | Stress (psi) | Strain | Stress (psi) | Strain | Average Stress (psi) | Average Strain |
|---|---|---|---|---|---|---|
| | Specimen 1 | | Specimen 2 | | | |
| 0 | 0 | 0 | 0 | 0 | 0 | 0 |
| 1 | 20363.64 | 0.001361 | 20363.64 | 0.000875 | 20363.60636 | 0.001118 |
| 2 | 40727.27 | 0.003189 | 40727.27 | 0.0024 | 40727.27273 | 0.0027945 |
| 2.5 | 50909.09 | 0.037862 | 50909.09 | - | 50909.09091 | 0.037862 |
| 2.76 | - | - | 56203.64 | 0.03686 | 56203.64 | 0.03686 |
| 3 | 61090.91 | 0.7339 | 61090.91 | - | 61909.90909 | 0.7339 |
| 3.15 | 64145.45 | 0.086298 | 64145.45 | - | 64145.45455 | 0.086298 |
| 3.5 | - | - | 71272.64 | 0.005309 | 71272.64 | 0.005309 |
| 3.64 | 74123.64 | - | 74123.64 | - | - | - |
| 3.84 | - | - | 78196.4 | - | - | - |

Table 3.17 - Description of specimen BS 6-1 – BS 6-3

| Description | BS 6-1 – BS 6-3 |
|---|---|
| Design mix | 1:0.7:1.7 |
| Silica fume | 25% by weight of cement |
| Viscocrete-1 | 4% by weight of cement |
| Mixing time | 10 minutes |
| Cover on sides | 1 inch |
| Cover from top/bottom | 1 inch |
| No of cylinders cast | 6 |
| W/C ratio | 0.22 |
| Steel ratio | 0.0646 |

| Materials | Quantity (kgs) |
|---|---|

| | |
|---|---|
| Cement | 279.6 |
| Fine aggregate/pan | 204.6/68.4 |
| Coarse aggregate | 642.6 |
| Water | 84.75 |
| Silica fume 25% | 96 |
| Viscorete-1 | 14.19 |

Table 3.18 - Description of material BS 6-1 – BS 6-3

Table 3.19 - Description of specimen BS 6-4 – BS 6-6

| **Description** | **BS 6-4 – BS 6-6** |
|---|---|
| Design mix | 1:0.7:1.7 |
| Silica fume | 15% by weight of cement |
| Viscocrete-1 | 4% by weight of cement |
| Mixing time | 10 minutes |
| Cover on sides | 1 inch |
| Cover from top/bottom | 1 inch |
| No of cylinders cast | 6 |
| W/C ratio | 0.23 |
| Steel ratio | 0.0646 |

Table 3.20 - Description of material BS 6-4 – BS 6-6

| **Materials** | **Quantity (kgs)** |
|---|---|
| Cement | 319.26 |
| Fine aggregate/pan | 204.6/68.4 |
| Coarse aggregate | 642.6 |
| Water | 86.388 |
| Silica fume 15% | 18.783 |
| Viscorete-1 | 14.19 |

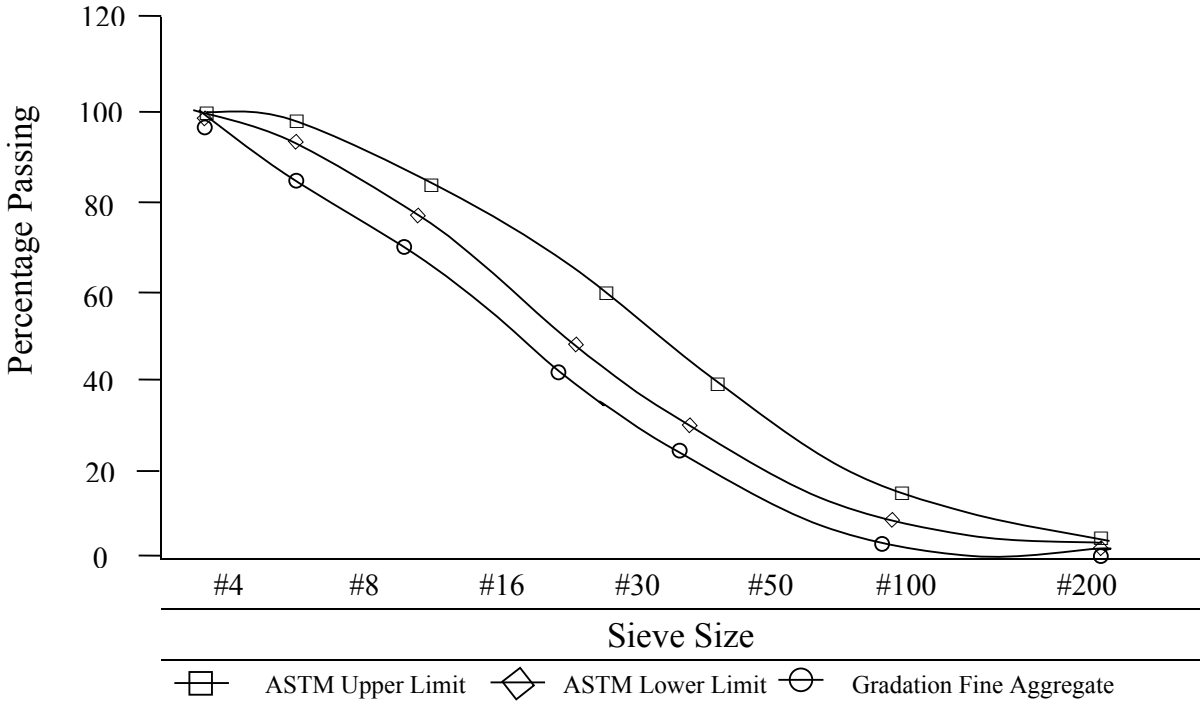


**Fig 3.1 - Particle size distribution of fine aggregate**

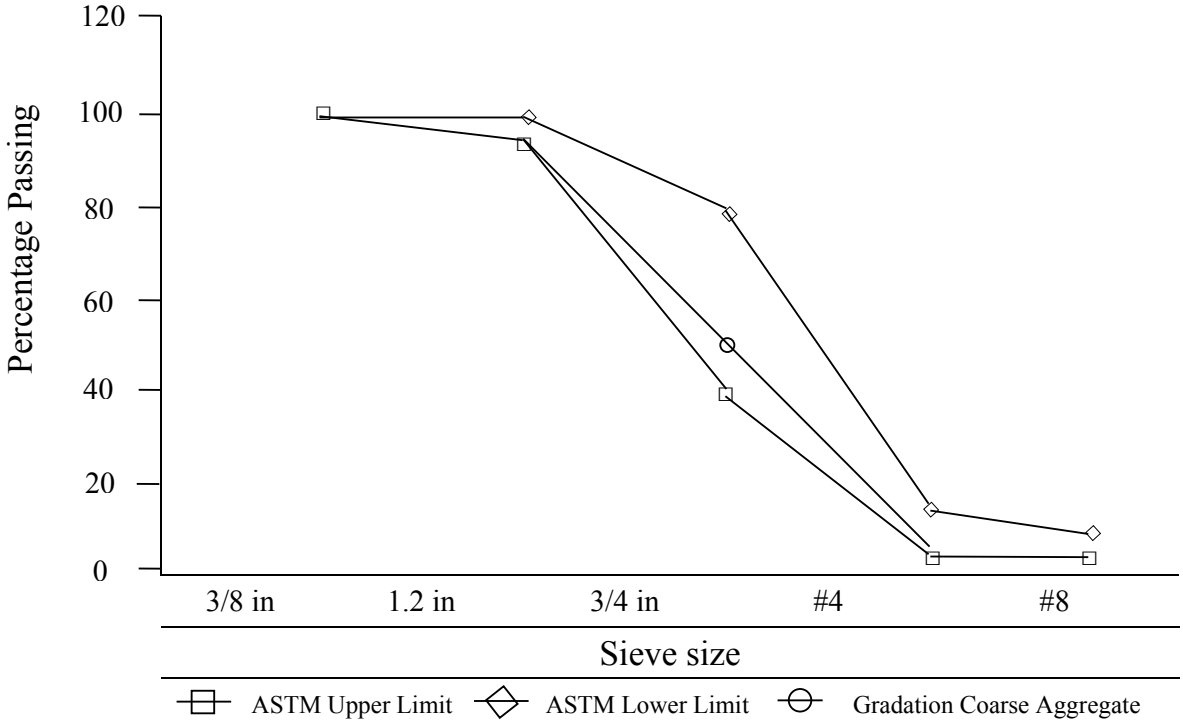


**Fig 3.2 - Particle size distribution of coarse aggregate**

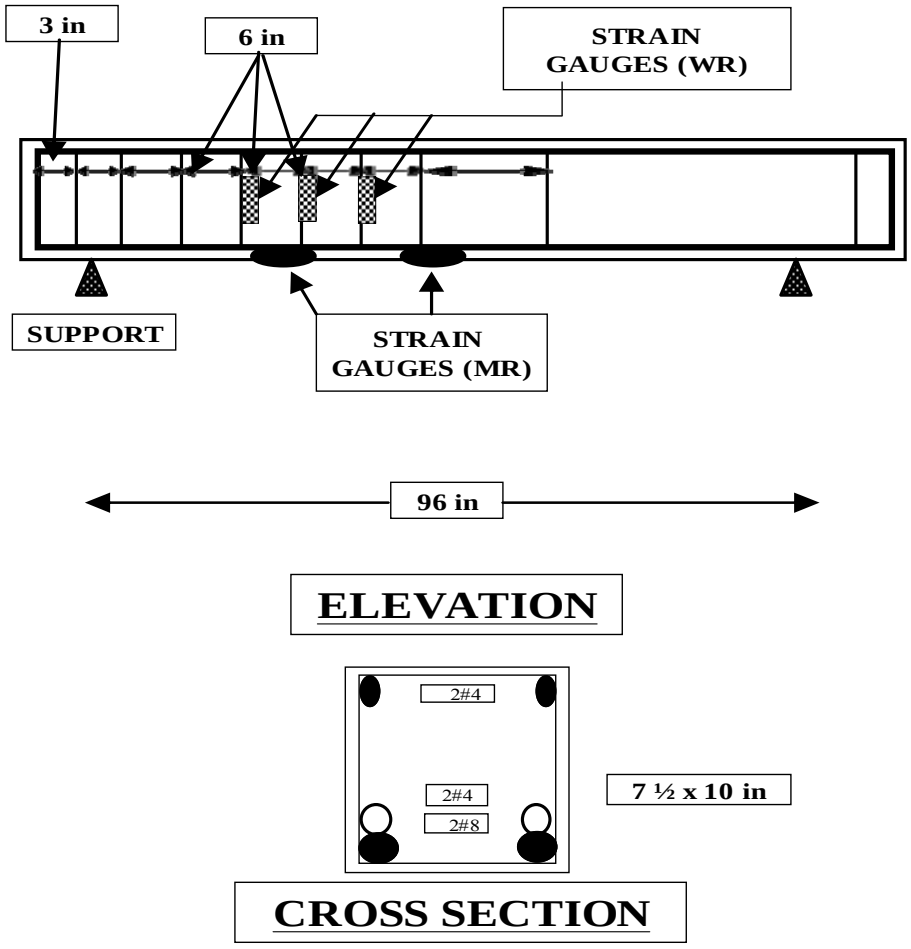


**Fig 3.3 - Cross section**

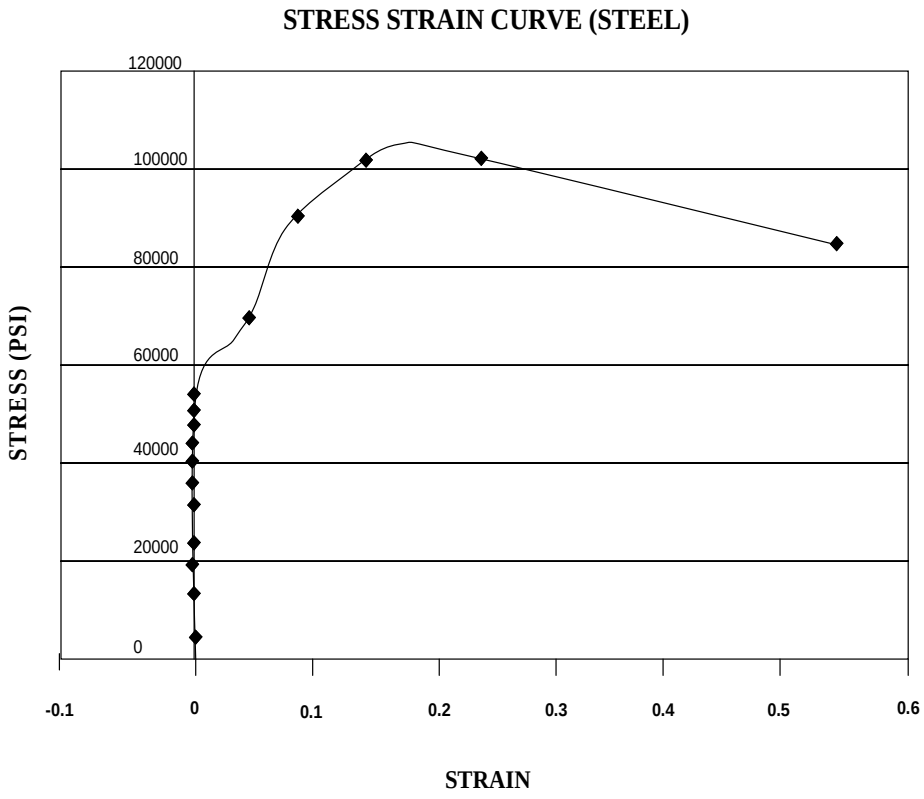


**Fig 3.4 - Stress strain curve**

**Fig 3.5 - Test setup**

+

# APPENDIX III

Table 4.1 - Compressive Strength on Day of Test BS 6-4

| Specimen | Size of cylinders (Inches) | Compressive strength |
|---|---|---|
| BS 6-4/4 | 6x12 | 9900 |
| BS 6-4/5 | “ | 9300 |
| BS 6-4/6 | “ | 9100 |
| Average | - | 9300 |

Table 4.2 - Compressive Strength on Day of Test BS 6-5

| Specimen | Size of cylinders (Inches) | Compressive strength |
|---|---|---|
| BS 6-5/4 | 6x12 | 9600 |
| BS 6-5/5 | “ | 9200 |
| BS 6-5/6 | “ | 9800 |
| Average | - | 9700 |

Table 4.3 - Compressive Strength on Day of Test BS 6-6

| Specimen | Size of cylinders (Inches) | Compressive strength |
|---|---|---|
| BS 6-6/4 | 6x12 | 9800 |
| BS 6-6/5 | “ | 9850 |
| BS 6-6/6 | “ | 9750 |
| Average | - | 9975 |

Table 4.4 - Load Deflection Data BS 6-1

| **Load (kn)** | **Deflection (mm)** |
|---|---|
| 0 | 0 |
| 40.03125 | 1.638 |
| 60.03125 | 3.02 |
| 80.0625 | 4.354 |
| 100.0313 | 5.64 |
| 120.0625 | 6.912 |
| 140.0625 | 8.164 |
| 160.0625 | 9.45 |
| 180.0625 | 10.746 |
| 200.0313 | 12.012 |
| 220.0313 | 13.532 |
| 240.0625 | 14.814 |
| 260.125 | 16.364 |
| 280.0313 | 17.702 |
| 300.0625 | 19.04 |
| 320.0625 | 20.384 |
| 340.0313 | 21.892 |
| 360.0938 | 23.882 |
| 380.0313 | 27.41 |
| 390.0625 | 31.03 |
| 395.3125 | 33.21 |
| 397.4375 | 34.472 |
| 392.9375 | 35.09 |
| 390.4688 | 35.116 |
| 360.375 | 35.264 |
| 345.375 | 35.78 |
| 305.012 | 35.85 |
| 280.25 | 35.95 |

Table 4.5 - Load Deflection Data BS 6-2

| **Load (kn)** | **Deflection (mm)** |
|---|---|
| 0 | 0 |
| 20.03125 | 4.112 |
| 40.09375 | 5.338 |
| 60.09375 | 6.704 |
| 80.03125 | 8.002 |
| 100.0313 | 9.282 |
| 120.0313 | 10.568 |
| 140.0313 | 12.172 |
| 160.0313 | 13.478 |
| 180.0313 | 15.166 |
| 200.0313 | 16.458 |
| 220.0313 | 17.796 |
| 240.0313 | 19.194 |
| 260.0313 | 20.718 |
| 280.0938 | 22.568 |
| 300.0625 | 24.778 |
| 320.0938 | 28.592 |
| 300.8438 | 44.91 |
| 280.375 | 50.828 |
| 290.0313 | 23.584 |
| 300.3125 | 24.866 |
| 310.1563 | 26.58 |
| 320.0313 | 28.63 |
| 329.4063 | 36.174 |
| 319.875 | 36.558 |
| 310.0313 | 37.416 |
| 300.9063 | 45.064 |
| 290.9375 | 48.34 |
| 280.6875 | 50.788 |
| 270.6563 | 53.204 |

Table 4.6 - Load Deflection Data BS 6-3

| **Load (kn)** | **Deflection (mm)** |
|---|---|
| 0 | 0 |
| 20.03125 | 2.526 |
| 40.125 | 3.904 |
| 60.03125 | 5.194 |
| 80 | 6.414 |
| 100 | 7.596 |
| 120 | 8.728 |
| 140 | 9.834 |
| 160 | 10.936 |
| 180 | 12.084 |
| 200 | 13.424 |
| 220 | 14.616 |
| 240 | 16.298 |
| 260 | 17.538 |
| 280 | 19.558 |
| 300 | 25.57 |
| 305.125 | 29.96 |
| 300.9688 | 35.12 |
| 295.6563 | 39.71 |
| 285 | 39.78 |
| 287.0938 | 42.134 |

Table 4.7 - Load Deflection Data BS 6-4

| **Load (kn)** | **Deflection (mm)** |
|---|---|
| 0 | 0 |
| 20 | 3.684 |
| 40 | 5.154 |
| 60 | 6.612 |
| 80 | 7.978 |
| 100 | 9.306 |
| 120 | 11.07 |
| 140 | 12.306 |
| 160 | 13.6 |
| 180.125 | 14.832 |
| 200 | 16.056 |
| 220 | 17.33 |
| 240 | 18.64 |
| 260 | 20.05 |
| 280 | 21.554 |
| 300 | 23.454 |
| 280.25 | 24.138 |
| 290.9063 | 22.432 |
| 300.5625 | 23.504 |
| 278.1875 | 24.138 |
| 250.9688 | 24.54 |
| 235.012 | 24.95 |
| 220.975 | 25.75 |

Table 4.8 - Load Deflection Data BS 6-5

| **Load (kn)** | **Deflection (mm)** |
|---|---|
| 0 | 0 |
| 20 | 3.314 |
| 40 | 4.606 |
| 60 | 5.876 |
| 80 | 7.178 |
| 100 | 8.45 |
| 120 | 9.686 |
| 140 | 11.122 |
| 160 | 12.32 |
| 180 | 13.528 |
| 200 | 14.858 |
| 220.0313 | 16.15 |
| 240 | 17.44 |
| 260 | 18.712 |
| 280 | 19.984 |
| 300 | 21.382 |
| 320 | 23.784 |
| 330 | 27.024 |
| 340 | 30.882 |
| 345.0313 | 33.486 |
| 349.25 | 35.51 |
| 335.012 | 35.65 |
| 320.075 | 36.01 |
| 305.789 | 36.75 |
| 290.125 | 37.314 |
| 275.789 | 37.95 |

Table 4.9 - Load Deflection Data BS 6-6

| **Load (kn)** | **Deflection (mm)** |
|---|---|
| 0 | 0 |
| 60.78125 | 2.09 |
| 80.09375 | 3.256 |
| 100.8438 | 4.31 |
| 120.0313 | 5.17 |
| 140.0313 | 6.002 |
| 160.9063 | 6.834 |
| 180.6875 | 7.61 |
| 200.9688 | 8.458 |
| 220.6875 | 9.404 |
| 240.7188 | 10.654 |
| 260.7188 | 11.806 |
| 280.6875 | 13.084 |
| 300.6875 | 14.384 |
| 320.1875 | 15.764 |
| 340.9688 | 17.692 |
| 360.7188 | 21.582 |
| 380.4688 | 32.654 |
| 400.3125 | 38.686 |
| 398.5938 | 40.242 |
| 396.9063 | 40.248 |
| 370.125 | 40.374 |
| 325.75 | 40.58 |

Table 4.10 - Load Strain Data BS 6-1

| **Load (kn)** | **Gauge 1 (mr)** | **Gauge 2 (wr)** |
|---|---|---|
| 0 | 2.54 | 0.9730 |
| 20 | 85.38 | 17.5210 |
| 40 | 213.46 | 41.3690 |
| 60 | 347.69 | 66.1920 |
| 80 | 481.94 | 79.8210 |
| 100 | 569.94 | 77.8740 |
| 120 | 695.10 | 72.0330 |
| 140 | 878.31 | 69.1120 |
| 160 | 982.16 | 62.2980 |
| 180 | 1065.15 | 62.7850 |
| 200 | 1342.73 | 61.8110 |
| 220 | 1967.72 | 65.7050 |
| 240 | 4201.64 | 69.5990 |
| 260 | 15078.52 | 77.3870 |
| 280 | 9741.53 | 86.6350 |
| 300 | - | 99.2910 |
| 320 | - | 129.9590 |
| 340 | - | 160.1410 |
| 360 | - | 178.6410 |
| 380 | - | 1574.9040 |
| 390.976 | - | 1886.96 |
| 395.898 | - | 1605.174 |
| 397.376 | - | 1426.514 |
| 392.145 | - | 1974.898 |
| 390.976 | - | 1884.029 |
| 360.149 | - | 164.036 |
| 345.136 | - | 147.971 |
| 305.510 | - | 91.99 |
| 280.1594 | - | 78.361 |

Table 4.11 - Load Strain Data BS 6-2

| **Load (kn)** | **Gauge 1 (mr)** | **Gauge 2 (wr)** | **Gauge 3 (wr)** |
|---|---|---|---|
| 0 | 0 | 0 | 0 |
| 0.0000 | 0.4932 | 0 | 0 |
| 20.0590 | 103.0916 | -0.488 | 0.488 |
| 40.0565 | 258.5086 | -0.488 | 5.3677 |
| 60.0540 | 434.7056 | -8.2955 | 8.2955 |
| 80.0515 | 615.4081 | -17.0789 | 12.6874 |
| 100.0490 | 796.175 | -18.5428 | 16.1032 |
| 120.0466 | 984.9132 | -18.0548 | 14.1513 |
| 140.0441 | 1207.3388 | -16.5909 | 3.9038 |
| 160.1031 | 1376.9422 | -12.6872 | 0 |
| 180.1006 | 1552.0442 | -10.7354 | 2.4399 |
| 200.0366 | 1731.6608 | -7.8076 | 7.8076 |
| 220.0341 | 1916.2918 | -1.9519 | 16.1032 |
| 240.0316 | 2097.0279 | 9.7596 | 27.327 |
| 260.0291 | 2361.0678 | 27.8154 | 49.7753 |
| 280.0266 | - | 44.8959 | 82.9616 |
| 300.0241 | - | 59.5367 | 163.008 |
| 320.0216 | - | 60.5128 | 222.0749 |
| 300.8855 | - | 254.7883 | 242.579 |
| 280.8880 | - | - | 458.4114 |

Table 4.12 - Load Strain Data BS 6-3

| **Load (kn)** | **Gauge 1 (mr)** | **Gauge 2 (wr)** | **Gauge 3 (wr)** |
|---|---|---|---|
| 0 | 0 | 0 | 0 |
| 20.05903646 | 103.0916 | -11.636 | -59.532 |
| 40.05653734 | 258.5086 | -12.606 | -148.329 |
| 60.05403822 | 434.7056 | -37.817 | -124.424 |
| 80.05154899 | 615.4081 | -59.148 | -111.251 |
| 100.2336467 | 796.175 | -70.783 | -102.957 |
| 120.1080863 | 984.9132 | -79.509 | -92.223 |
| 140.0440615 | 1207.3388 | -89.204 | -23.911 |
| 160.0415624 | 1376.9422 | -95.506 | -35.135 |
| 180.0390633 | 1552.0442 | -104.716 | -30.255 |
| 200.0365741 | 1731.6608 | -99.869 | -14.152 |
| 220.0340749 | 1916.2918 | -95.991 | -23.911 |
| 240.0315758 | 2097.0279 | -65.935 | 2.44 |
| 260.0290866 | 2361.0678 | -8.242 | 92.24 |
| 280.0881132 | - | 32.486 | 130.312 |
| 300.0400921 | - | 112.984 | - |
| 305.0400921 | - | 112.986 | - |
| 295.1631533 | - | 111.042 | - |
| 285.0105837 | - | 57.7 | - |
| 287.9025285 | - | 73.702 | - |

Table 4.13 - Load Strain Data BS 6-4

| Load (kn) | Gauge 1 (mr) | Gauge 2 (mr) | Gauge 3 (wr) | Gauge 4 (wr) |
|---|---|---|---|---|
| 0 | 0 | 0 | 0 | 0 |
| 20.18210 | 78.9149 | 21.6537 | 43.7068 | 26.3627 |
| 40.05654 | 279.9339 | 111.2858 | 115.9049 | 299.8348 |
| 60.05404 | 431.9771 | 1771.4316 | -358.8419 | 471.8076 |
| 80.05155 | 581.1219 | 581.1219 | -474.6379 | 402.4252 |
| 100.04905 | 729.82 | 931.3408 | 1446.7846 | 693.7001 |
| 120.04655 | 878.0709 | 518.1374 | 4460.3088 | 600.3369 |
| 140.04406 | 1040.1166 | 1054.8852 | 373.8395 | 2731.4569 |
| 160.04156 | 1178.142 | 5469.0632 | 23.0806 | 1450.0406 |
| 180.03907 | 1312.7653 | 6044.5299 | 573.8909 | 1993.2894 |
| 200.03657 | 1439.0687 | 8820.229 | -3677.423 | 1485.782 |
| 220.03407 | 1628.8288 | 10648.3794 | -3650.1223 | 2148.6809 |
| 240.03158 | 1831.4493 | 12203.9332 | -3595.5165 | 10622.9075 |
| 260.02908 | 2094.1899 | - | -3569.1866 | 5117.1367 |
| 280.02659 | 2129.1338 | - | -3606.2431 | 9348.76 |
| 300.08562 | 2241.8568 | - | -3570.1618 | 10164.4644 |
| 280.37323 | 2182.2926 | - | -3557.4839 | 7534.9199 |
| 300.14715 | 2243.3337 | - | -3575.0378 | 10168.4491 |
| 278.27421 | 2097.1428 | - | -3572.1122 | 6729.8543 |
| 250.79946 | 1998.7215 | - | -3574.0626 | 4475.4546 |
| 235.17065 | 1909.6668 | - | -3583.8145 | 3106.5942 |
| 220.09560 | 1851.6174 | - | -3594.5413 | 2513.0824 |

Table 4.14 - Load Strain Data BS 6-5

| Load (kn) | Gauge1 (mr) | Gauge 2 (mr) | Gauge 3 (wr) | Gauge 4 (wr) | Gauge 5 (wr) |
|---|---|---|---|---|---|
| 0 | 0 | 0 | 0 | 0 | 0 |
| 20.05903 | 61.128 | 66.4917 | 11.734 | 0.3041 | 1.5245 |
| 40.05654 | 148.6762 | 188.7154 | 30.8024 | 10.9472 | 18.8022 |
| 60.05404 | 219.6063 | 351.1267 | 53.7832 | 24.6315 | 37.097 |
| 80.05155 | 284.1859 | 543.5706 | 79.21 | 33.7546 | 54.8841 |
| 100.0491 | 346.8163 | 728.8894 | 104.638 | 43.7902 | 72.6719 |
| 120.0466 | 401.135 | 937.0789 | 127.1332 | 54.7383 | 85.8861 |
| 140.0441 | 439.7978 | 1114.1372 | 143.2716 | 65.3826 | 115.8734 |
| 160.0416 | 478.953 | 1287.0537 | 159.8996 | 68.4238 | 145.8624 |
| 180.0391 | 514.1952 | 1472.6443 | 179.4627 | 84.8469 | 271.4286 |
| 200.0366 | 537.202 | 1693.7598 | 194.6246 | 91.2338 | 360.9197 |
| 220.0341 | 559.7202 | 1874.0883 | 211.2543 | 97.3167 | 543.0007 |
| 240.0931 | 571.9588 | 2002.7618 | 226.9062 | 100.9664 | 702.756 |
| 260.0291 | 583.7081 | 2130.8664 | 242.0696 | 104.9203 | 874.2685 |
| 280.0266 | 591.5411 | 2312.5537 | 257.7225 | 109.4825 | 1023.9432 |
| 300.0241 | 595.4577 | 2499.7234 | 272.8868 | 104.0079 | 1306.1018 |
| 320.0216 | - | 2781.5107 | 307.1303 | 99.1415 | 2876.5848 |
| 340.0191 | - | 3421.5313 | 306.6411 | 104.0079 | - |
| 320.6984 | - | 3473.395 | 307.6195 | 97.9249 | - |

Table 4.15 - Load Strain Data BS 6-6

| **Load (kn)** | **Gauge 1 (mr)** | **Gauge 2 (wr)** | **Gauge 3 (wr)** |
|---|---|---|---|
| 0 | 0 | 0 | 0 |
| 20.05903 | 45.50883 | 16.3872 | 120.76 |
| 40.9795 | 105.36905 | 27.8089 | 180.651 |
| 60.05404 | 154.84564 | 42.70715 | 225.031 |
| 80.05155 | 207.79094 | 61.5789 | 244.93837 |
| 100.0491 | 277.07351 | 97.83449 | 270.654 |
| 120.0466 | 361.21506 | 148.00059 | 306.06929 |
| 140.0441 | 453.29181 | 197.67487 | 366.22935 |
| 160.0416 | 575.0964 | 248.84447 | 413.18853 |
| 180.0391 | 656.81099 | 264.74286 | 448.41078 |
| 200 | 682.07089 | 272.69225 | - |

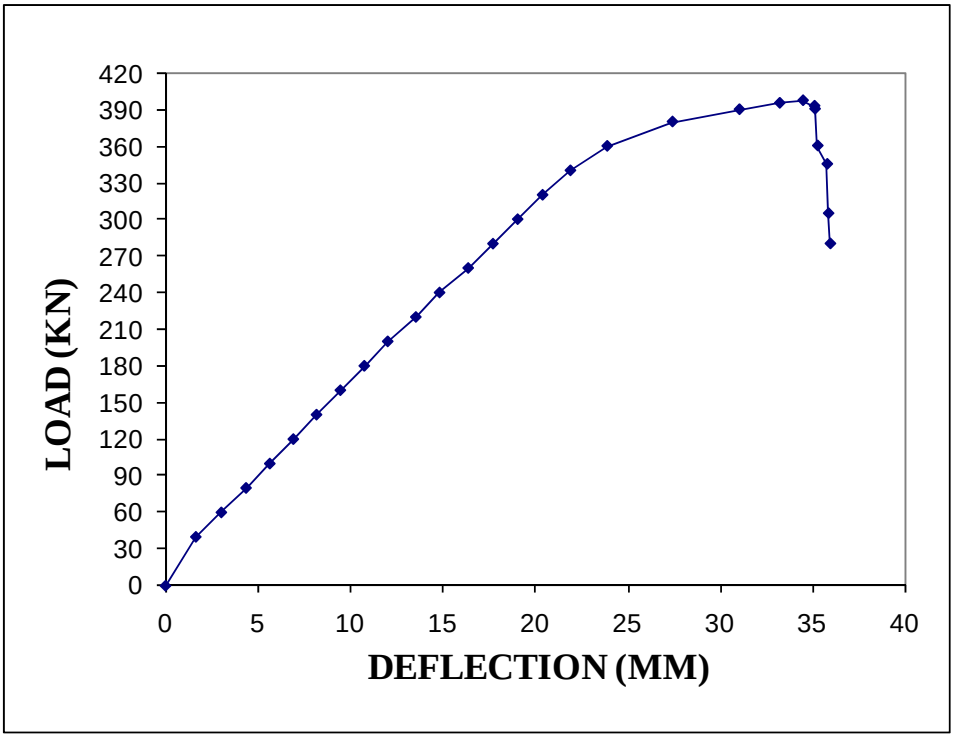


Fig 4.1 - Load deflection behavior BS 6-1

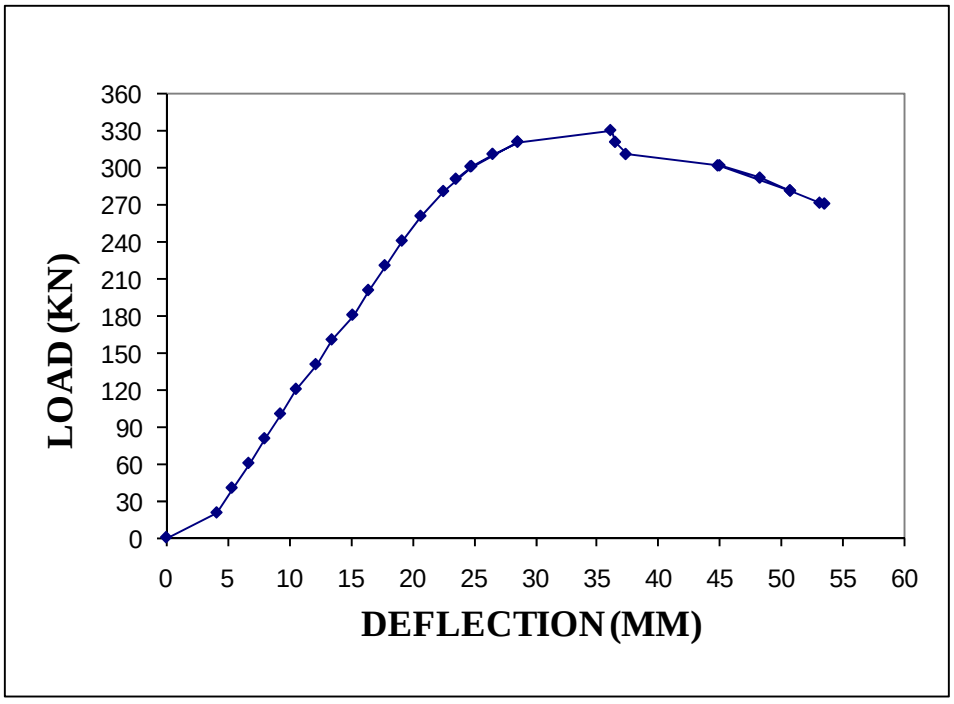


Fig 4.2 - Load deflection behavior BS 6-2

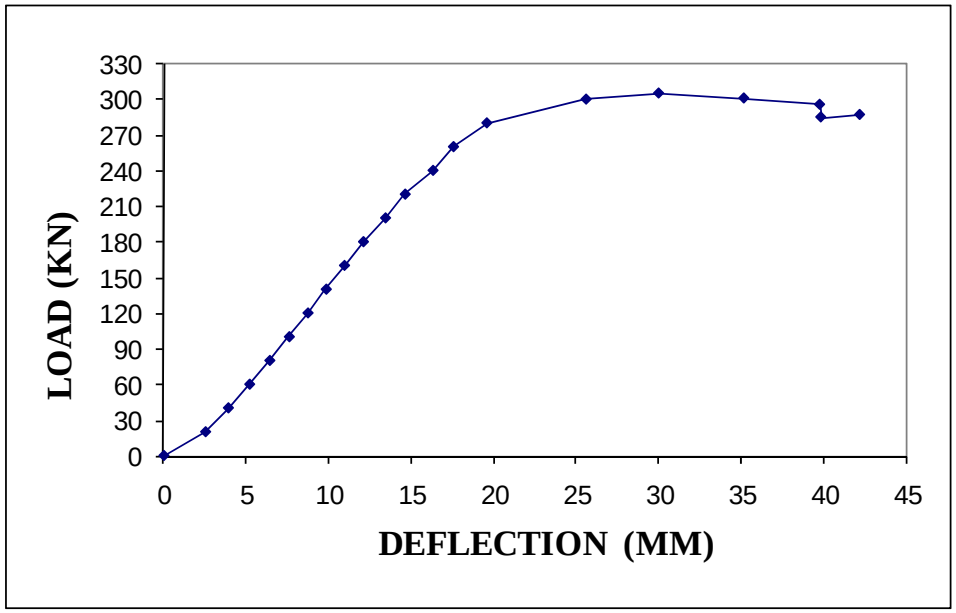


Fig 4.3 - Load deflection behavior BS 6-3

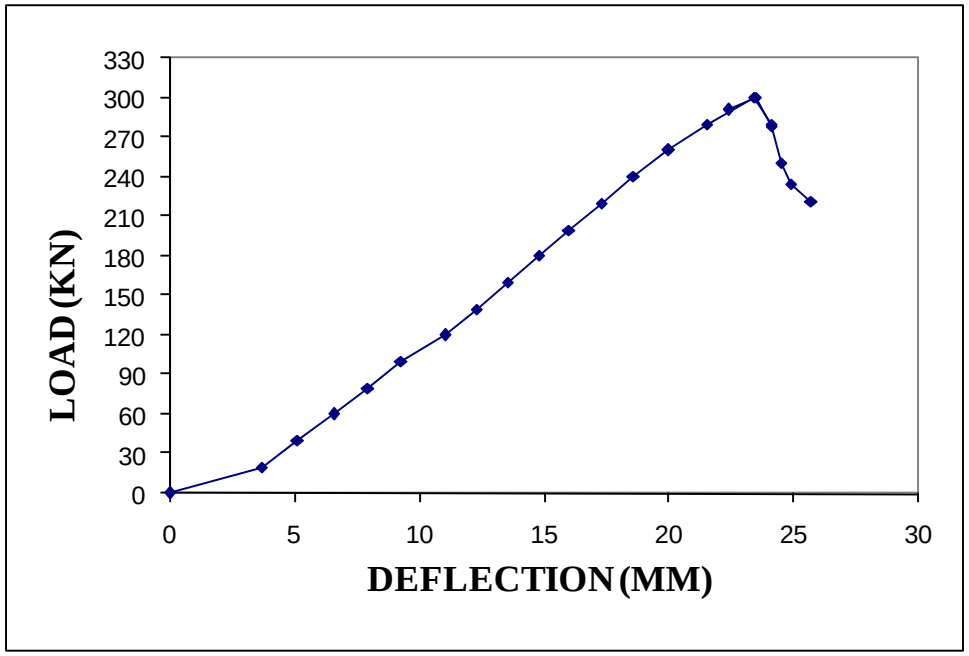


Fig 4.4 - Load deflection behavior BS 6-4

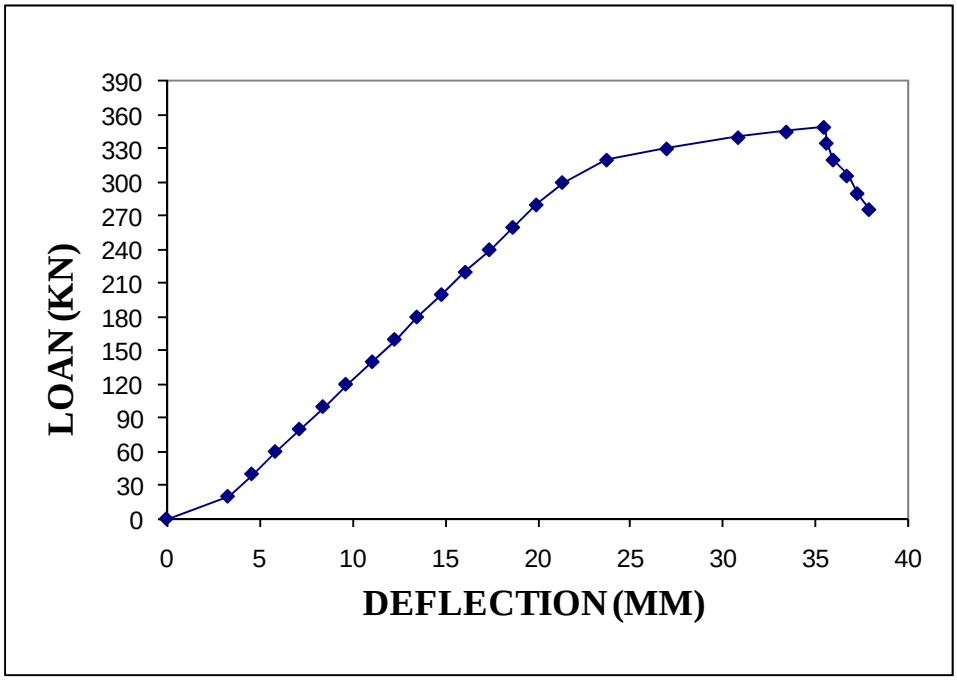


Fig 4.5 - Load deflection behavior BS 6-5

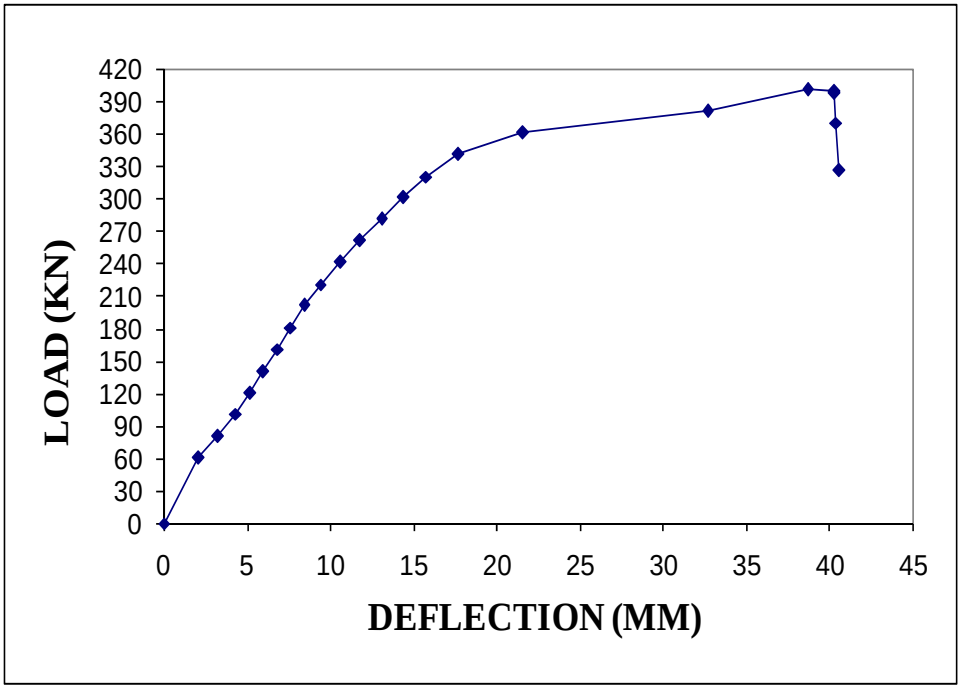


Fig 4.6 - Load deflection behavior BS 6-6

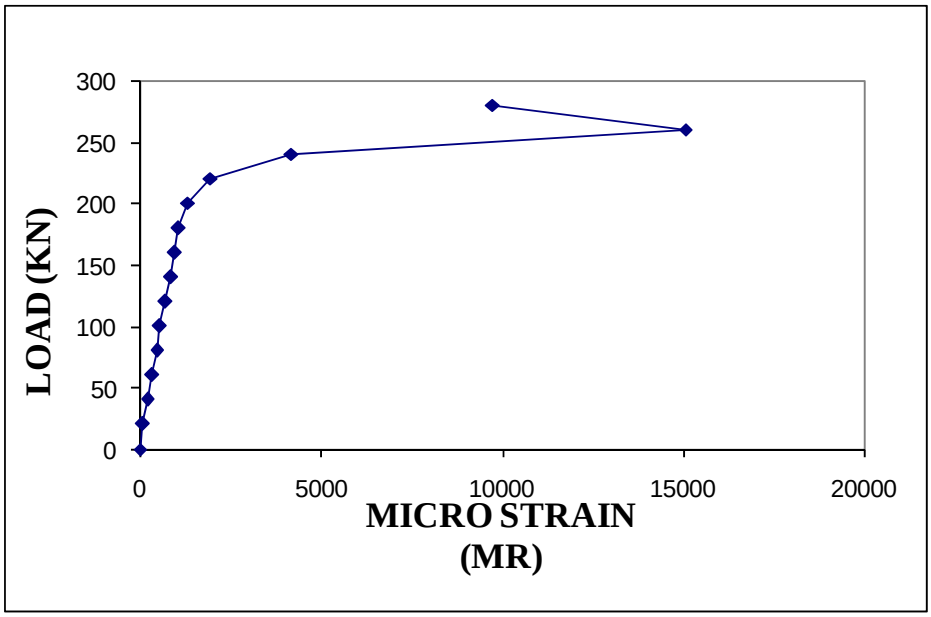


Fig 4.7 (a) - Load strain behavior BS 6-1

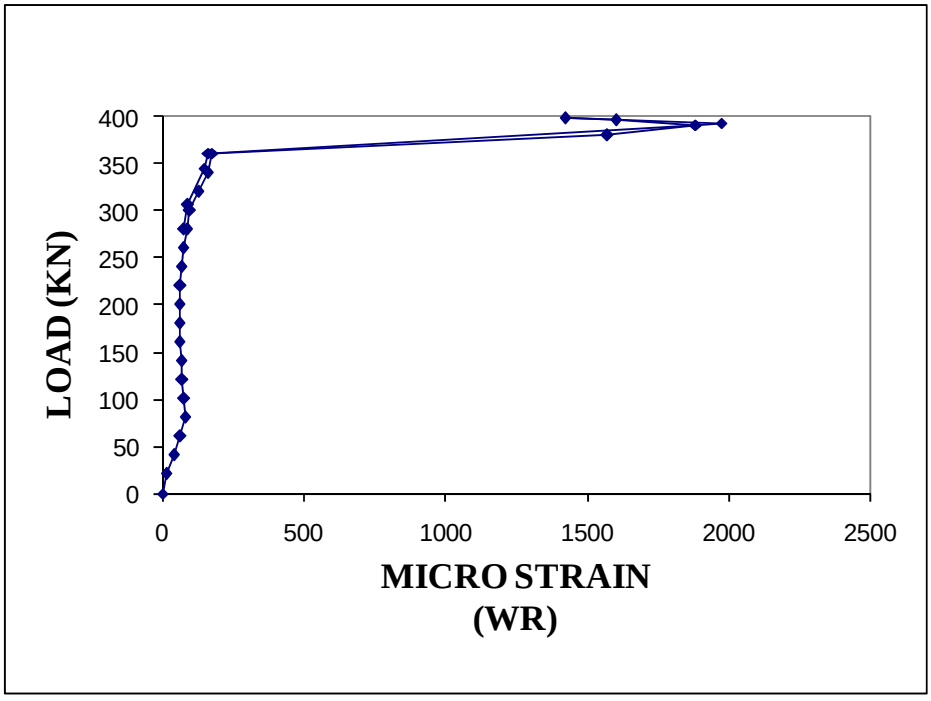


Fig 4.7 (b) - Load strain behavior BS 6-1

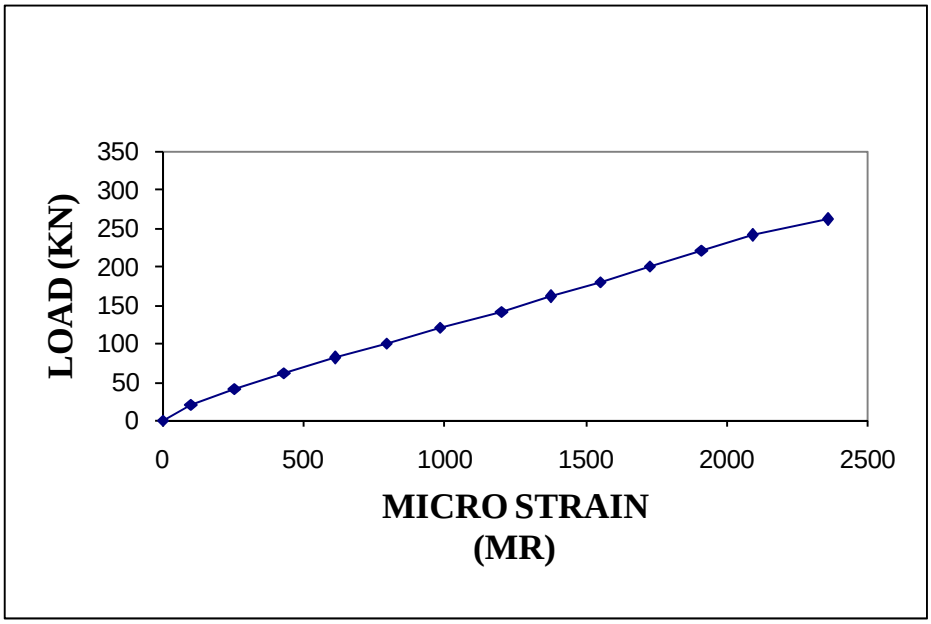


Fig 4.8 (a) - Load strain behavior BS 6-2

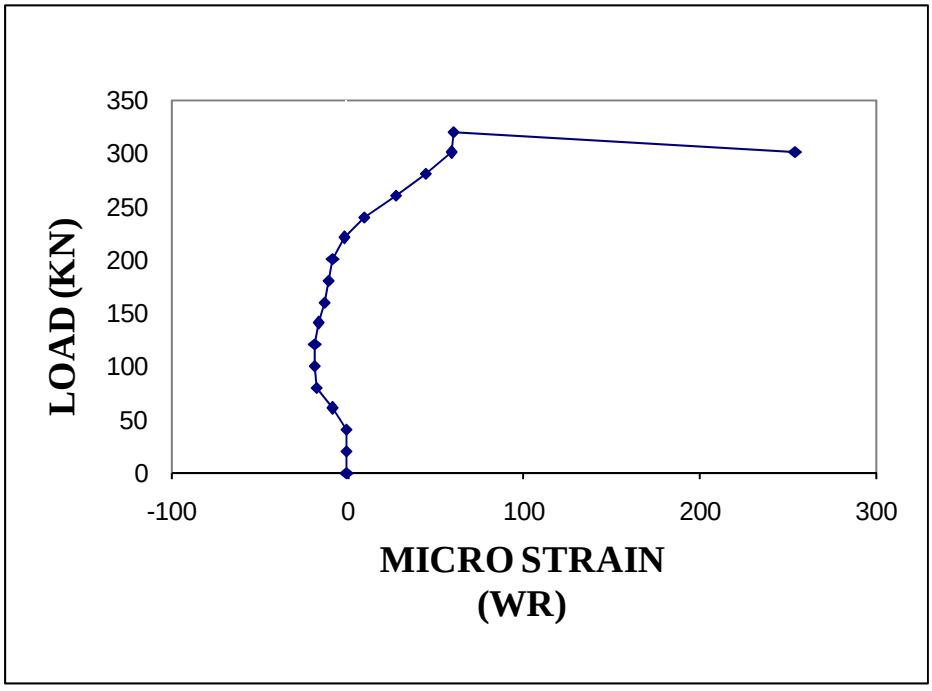


Fig 4.8 (b) - Load strain behavior BS 6-2

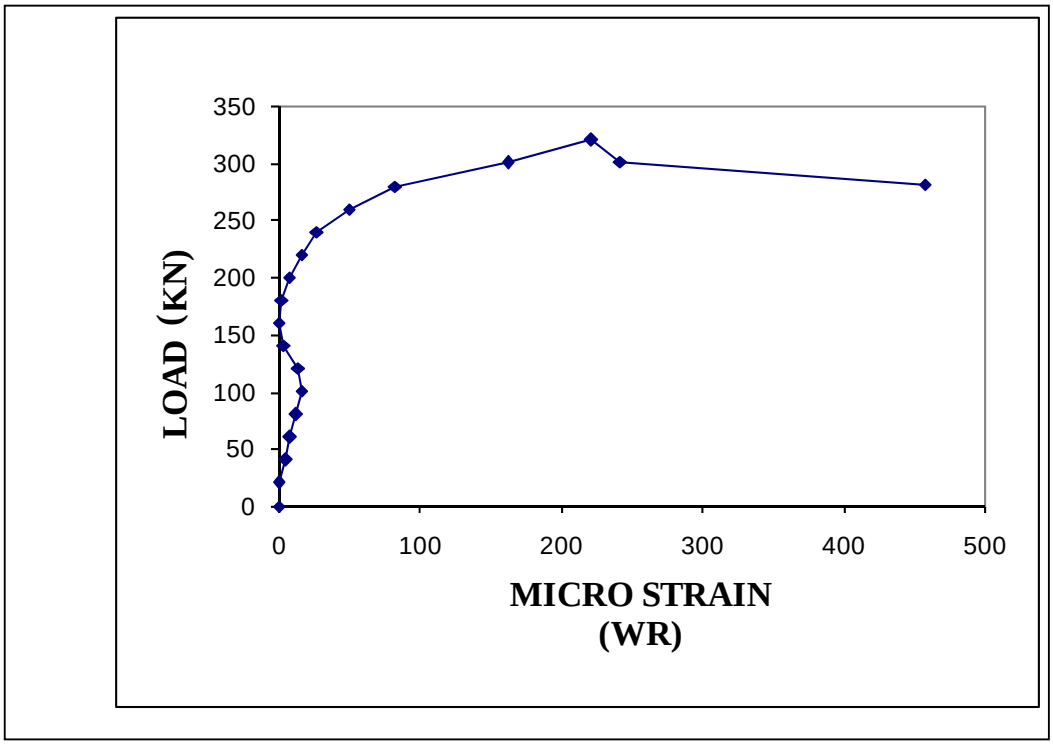


Fig 4.8 (c) - Load strain behavior BS 6-2

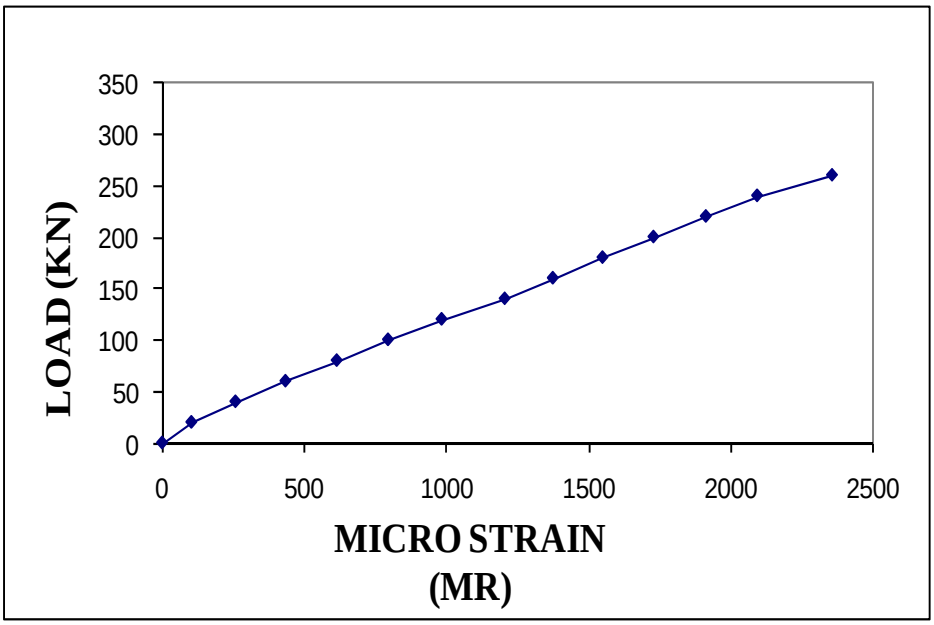


Fig 4.9 (a) - Load strain behavior BS 6-3

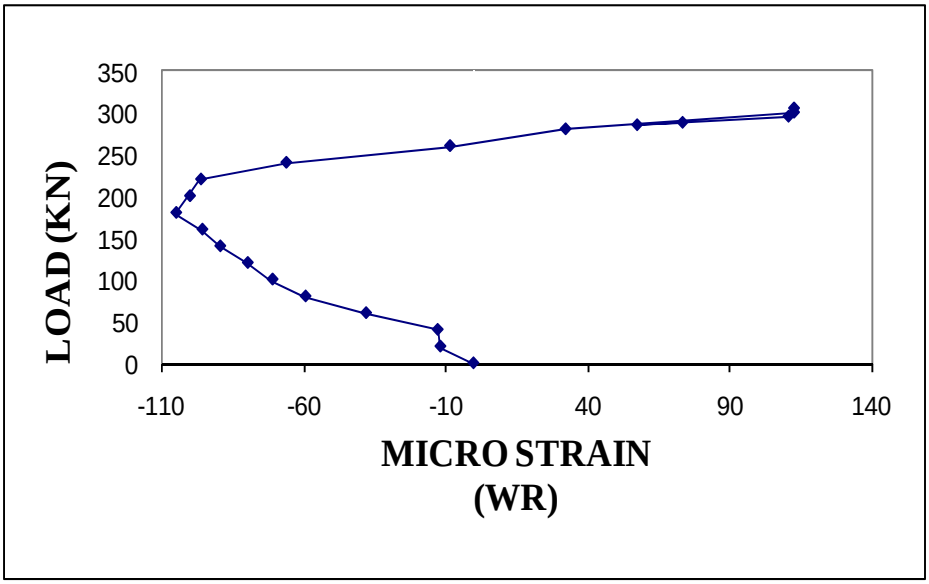


Fig 4.9 (b) - Load strain behavior BS 6-3

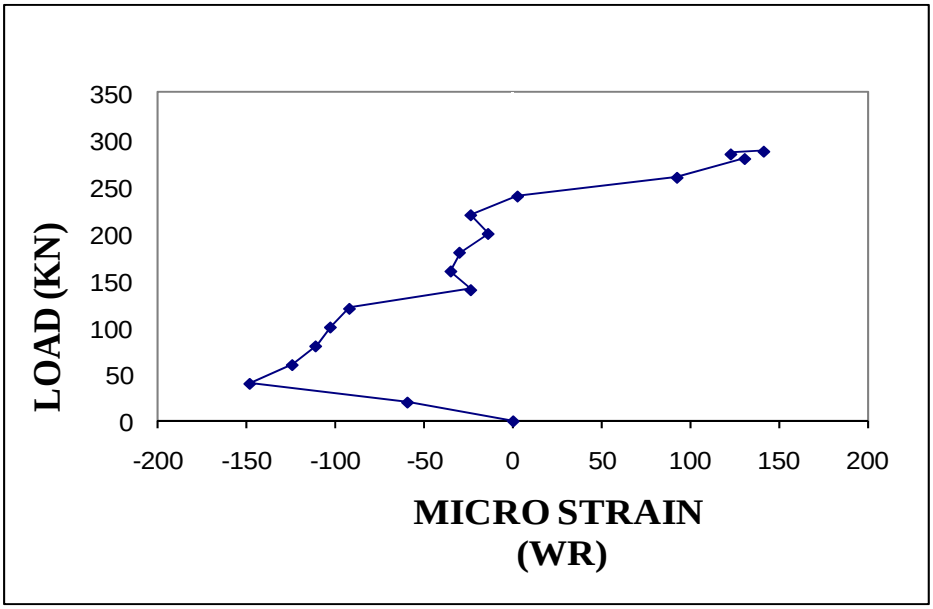


Fig 4.9 (c) - Load strain behavior BS 6-3

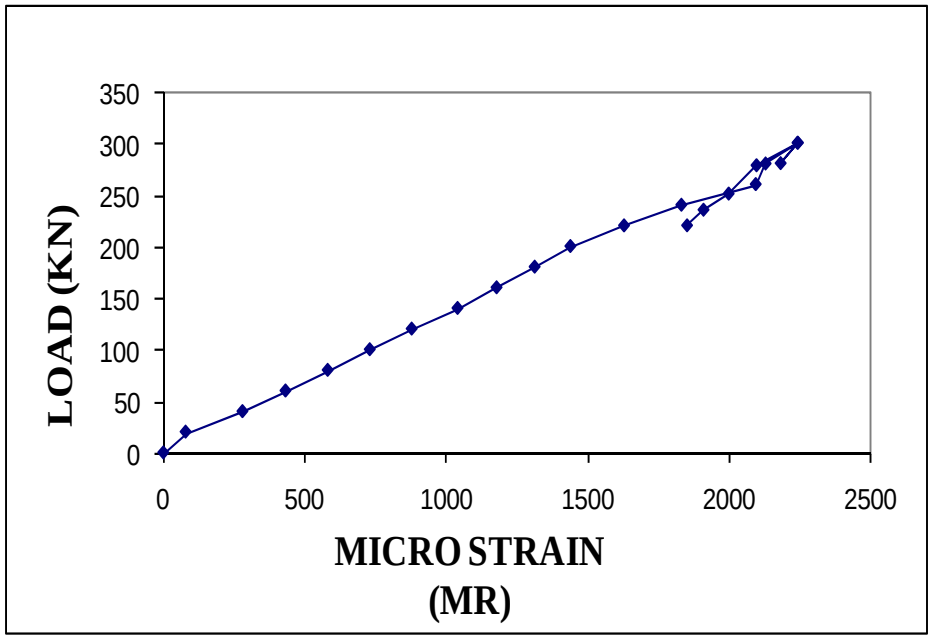


Fig 4.10 (a) - Load strain behavior BS 6-4

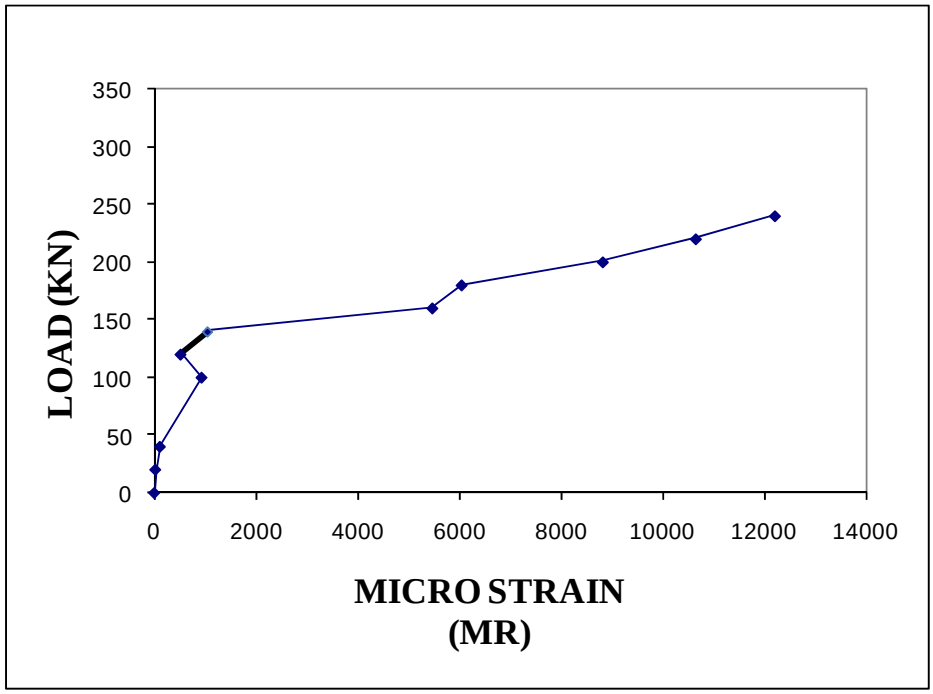


Fig 4.10 (b) - Load strain behavior BS 6-4

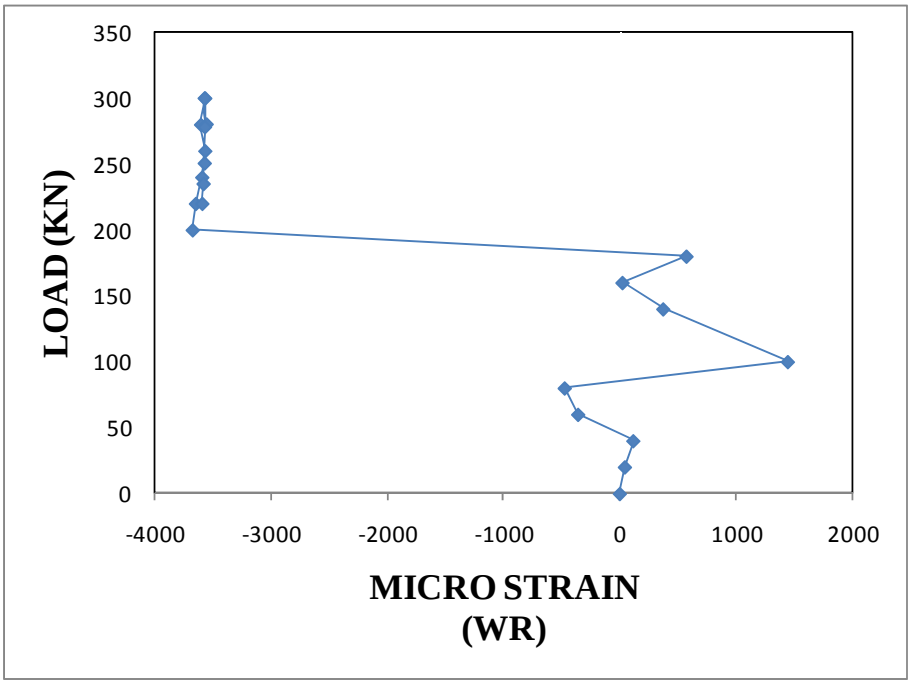


Fig 4.10 (c) - Load strain behavior BS 6-4

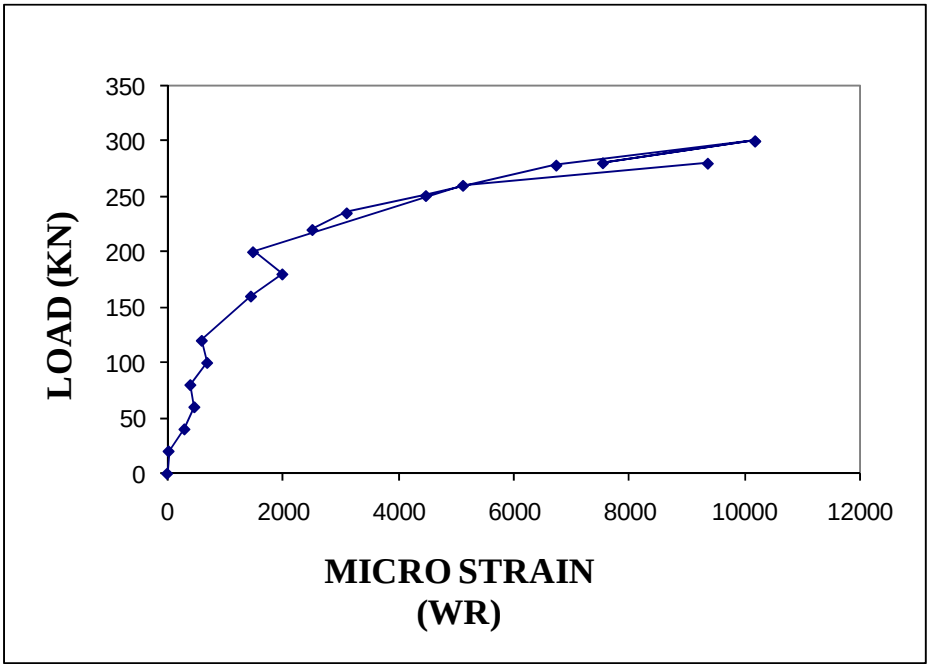


Fig 4.10 (d) - Load strain behavior BS 6-4

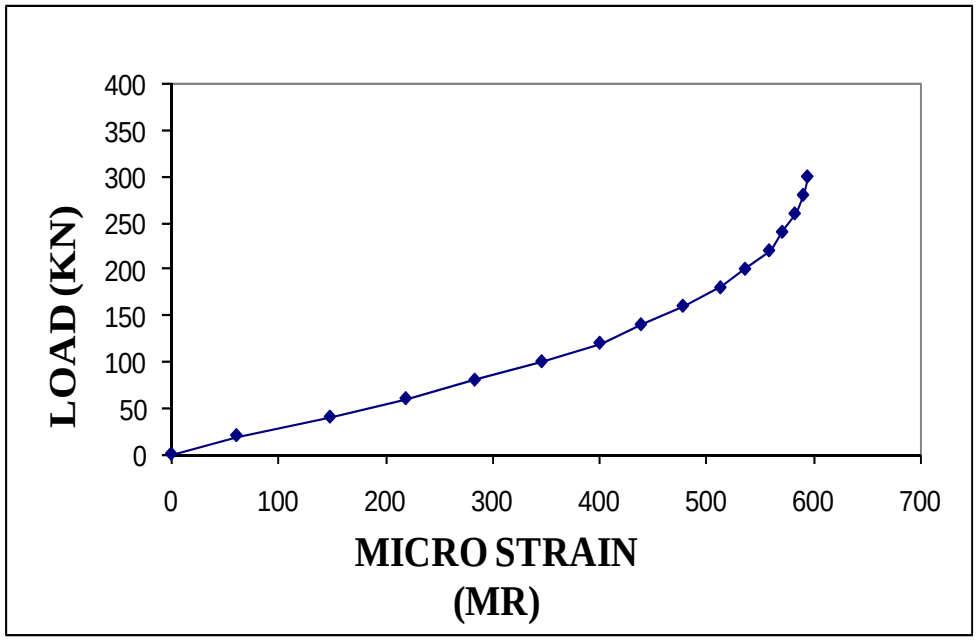


Fig 4.11 (a) - Load strain behavior BS 6-5

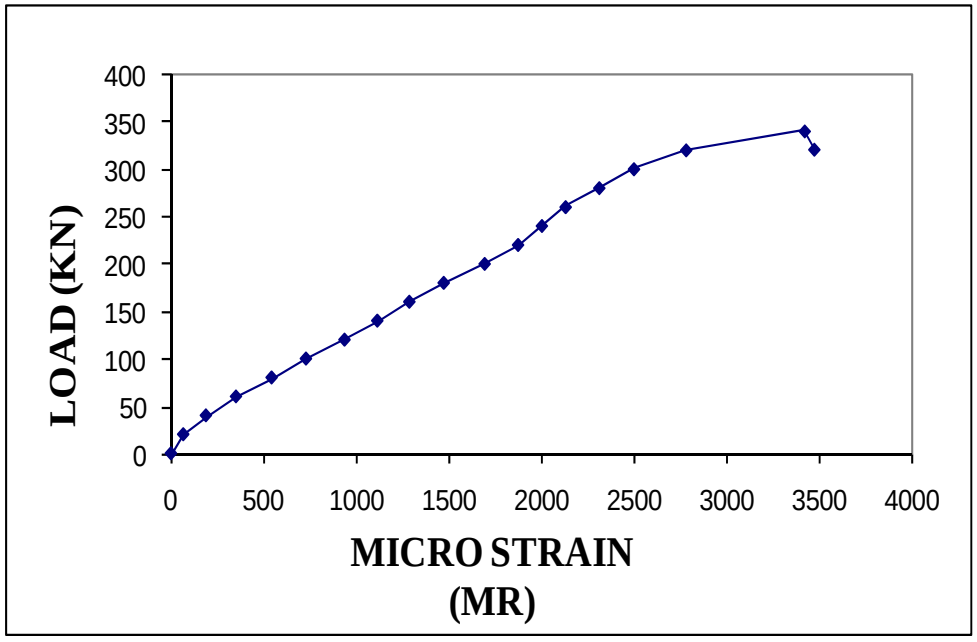


Fig 4.11 (b) - Load strain behavior BS 6-5

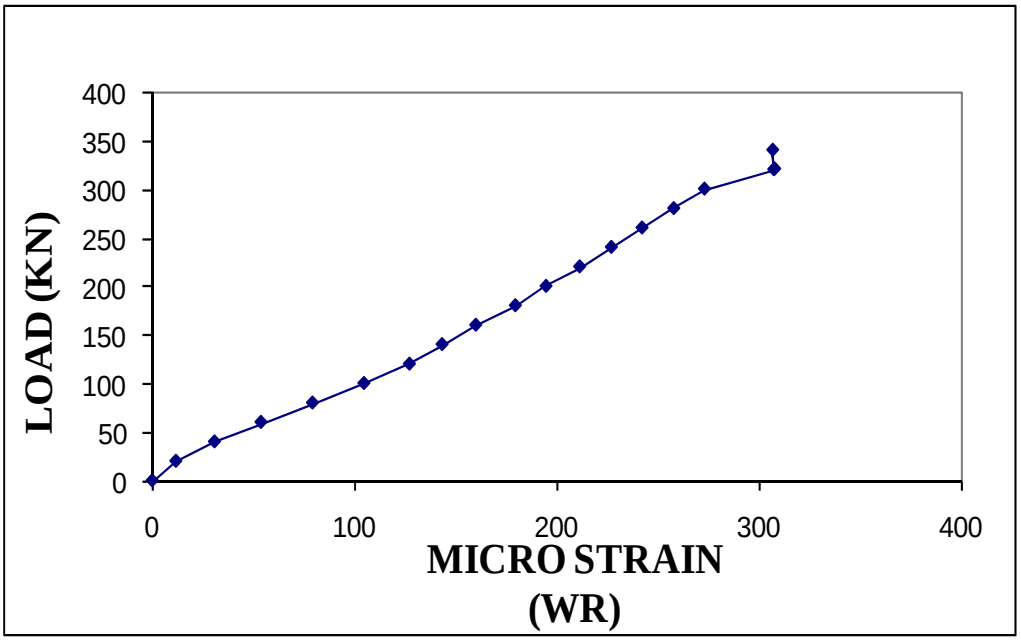


Fig 4.11 (c) - Load strain behavior BS 6-5

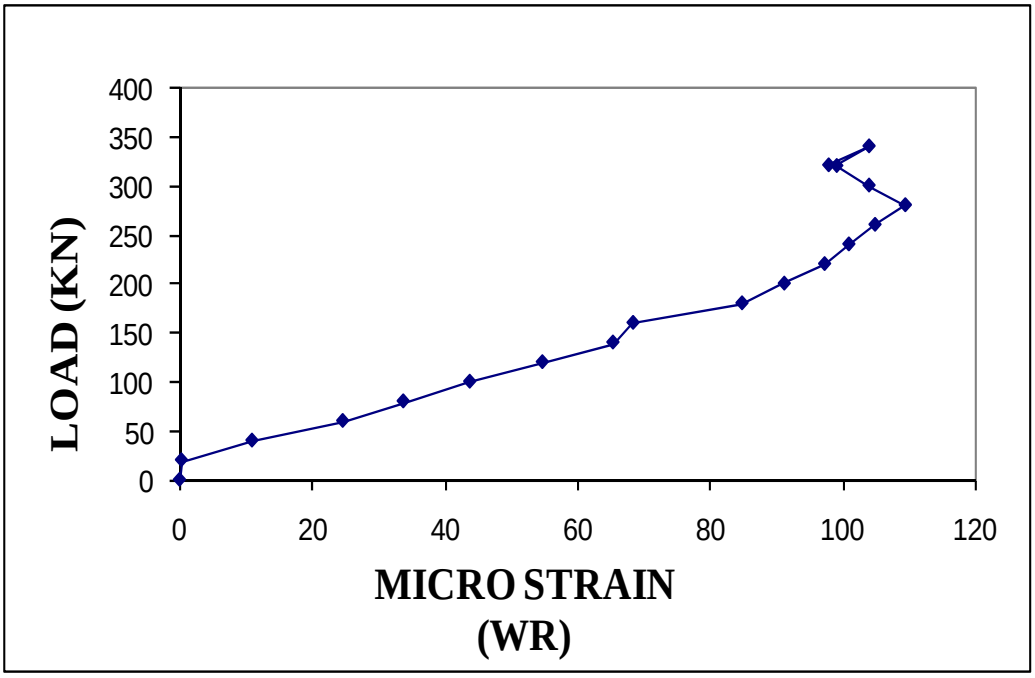


Fig 4.11 (d) - Load strain behavior BS 6-5

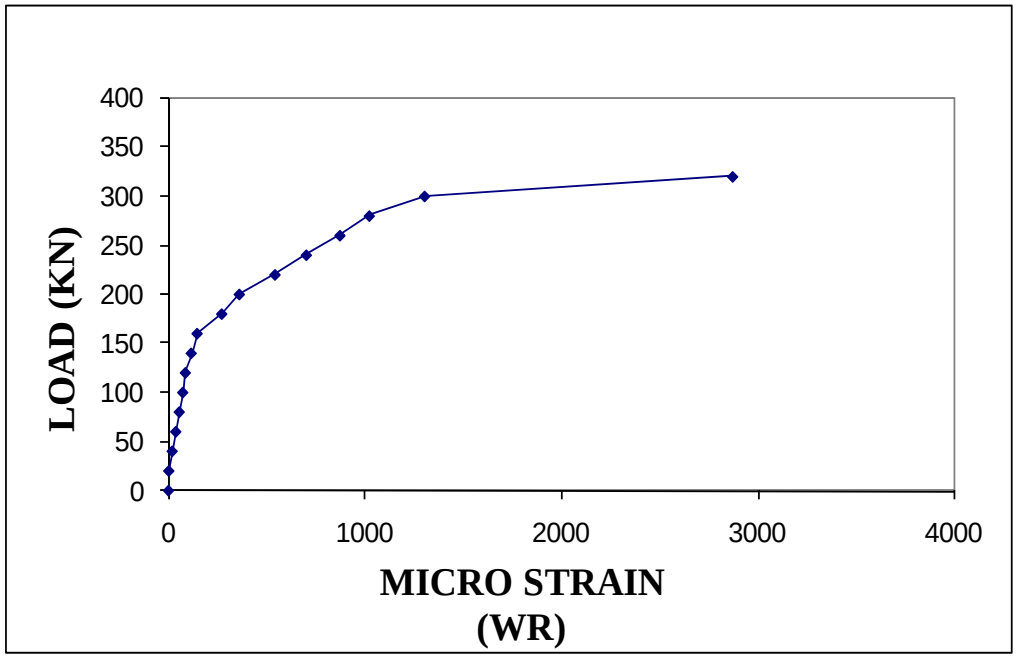


Fig 4.11 (e) - Load strain behavior BS 6-5

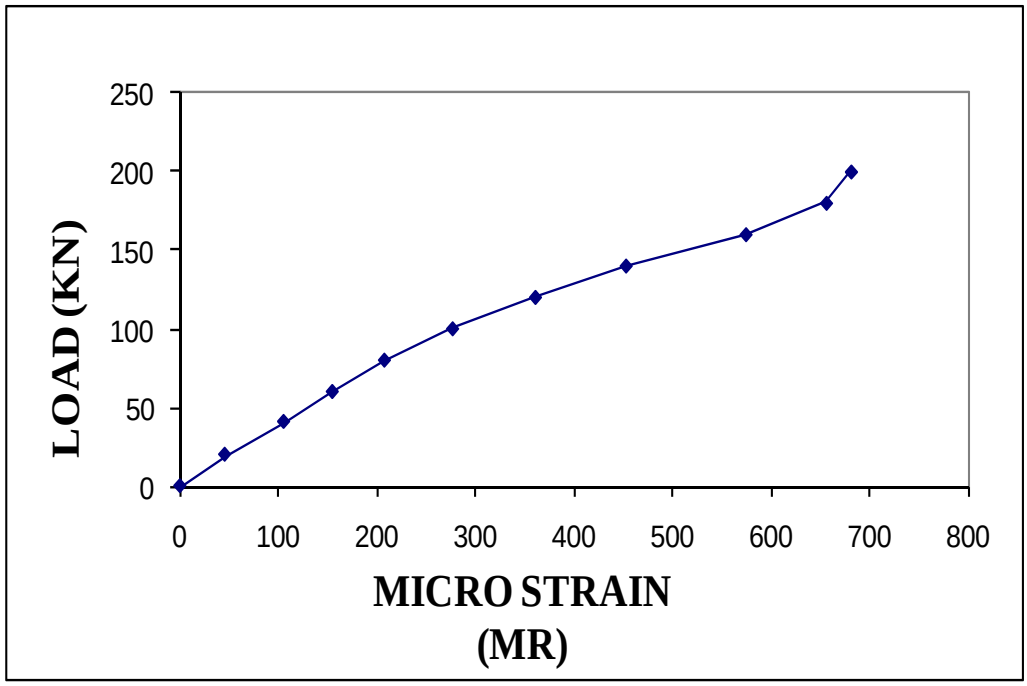


Fig 4.12 (a) - Load strain behavior BS 6-6

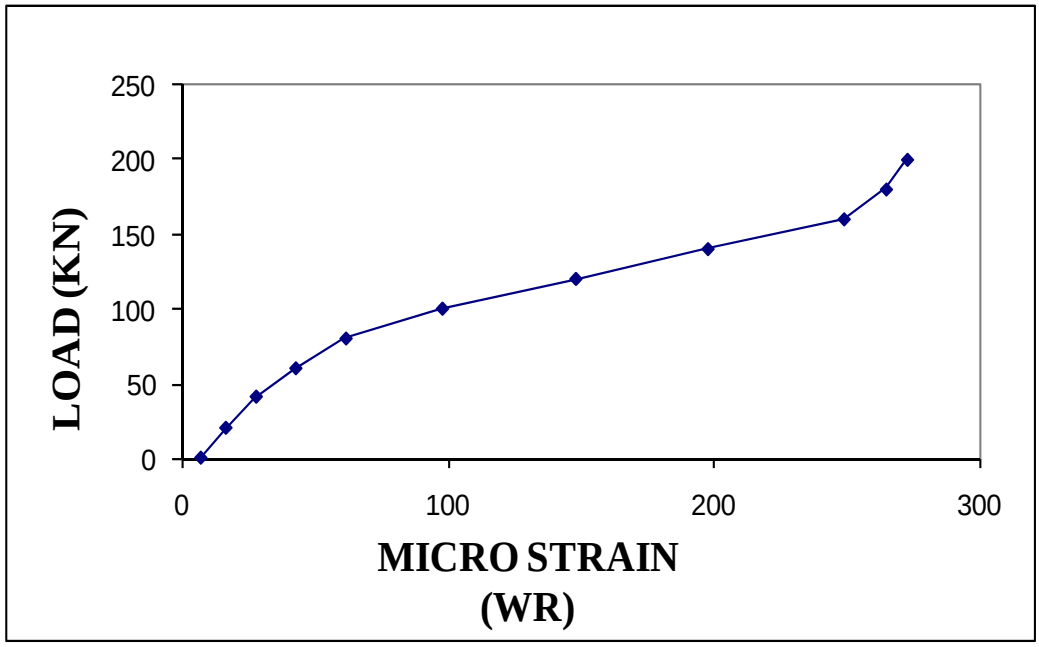


Fig 4.12 (b) - Load strain behavior BS 6-6

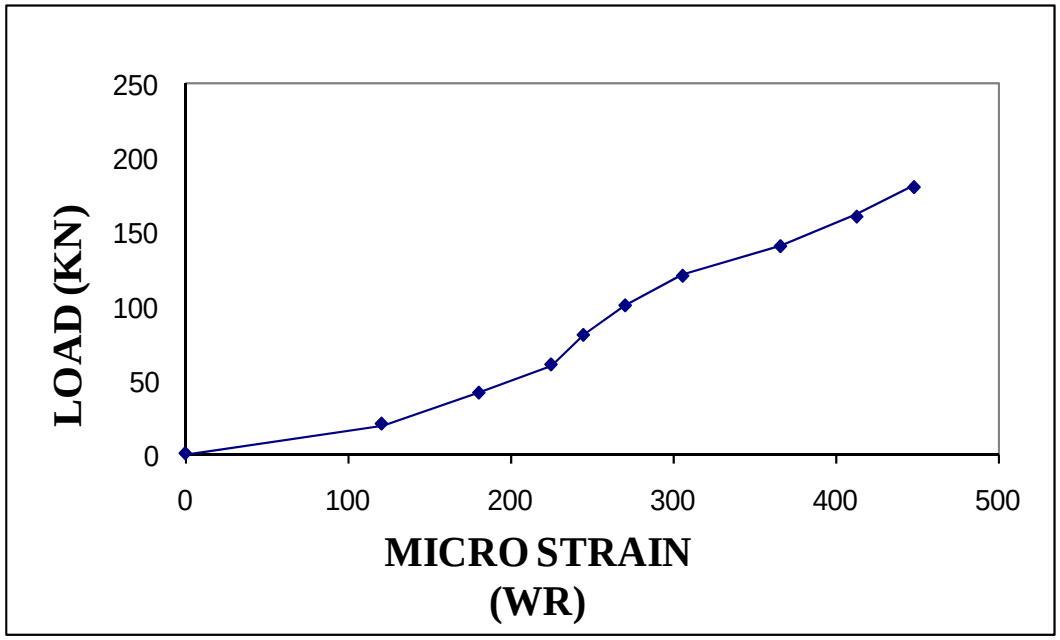


Fig 4.12 (c) - Load strain behavior BS 6-6


Fig 4.13 (a) - Cracking pattern BS 6-1

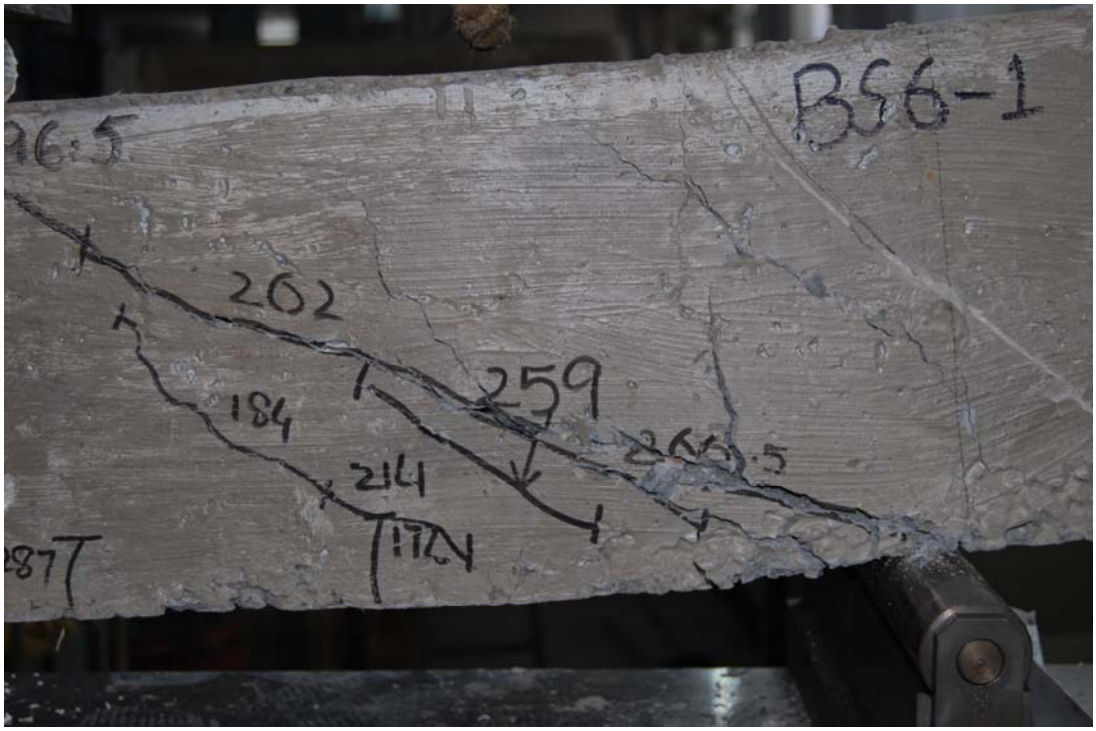


Fig 4.13 (b) - Cracking pattern BS 6-1

Fig 4.14 (a) - Cracking pattern BS 6-2


Fig 4.14 (b) - Cracking pattern BS 6-2

Fig 4.15 - Cracking pattern BS 6-3


Fig 4.16 - Cracking pattern BS 6-4

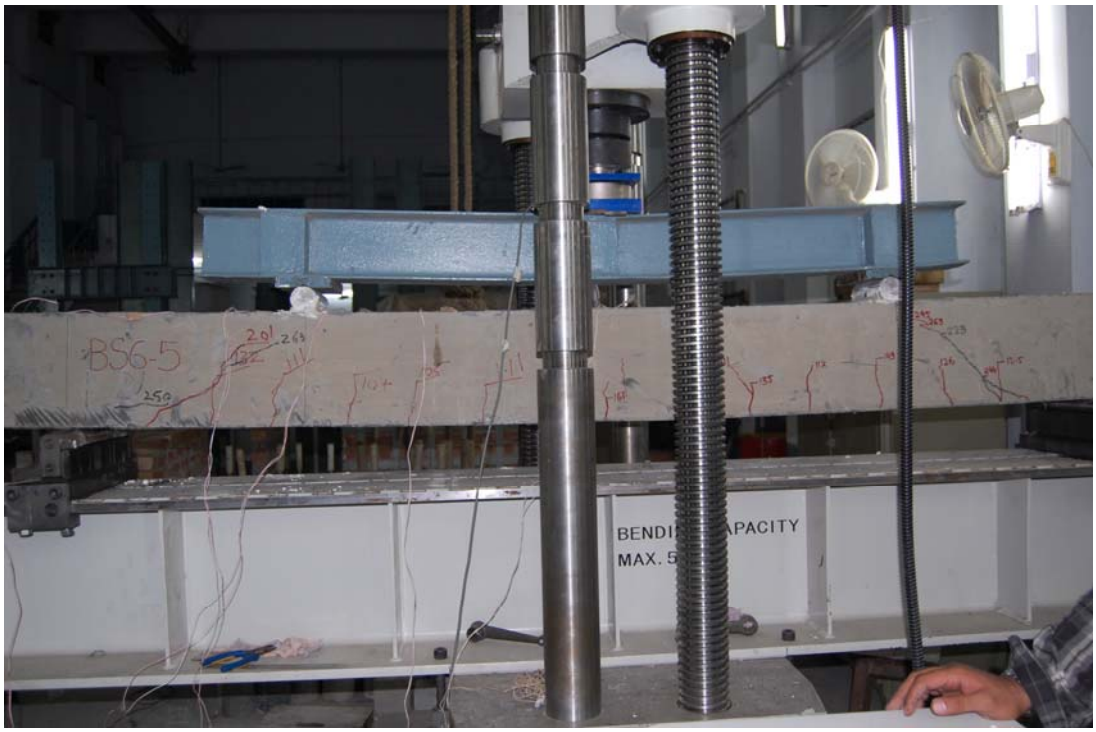


Fig 4.17 - Cracking pattern BS 6-5

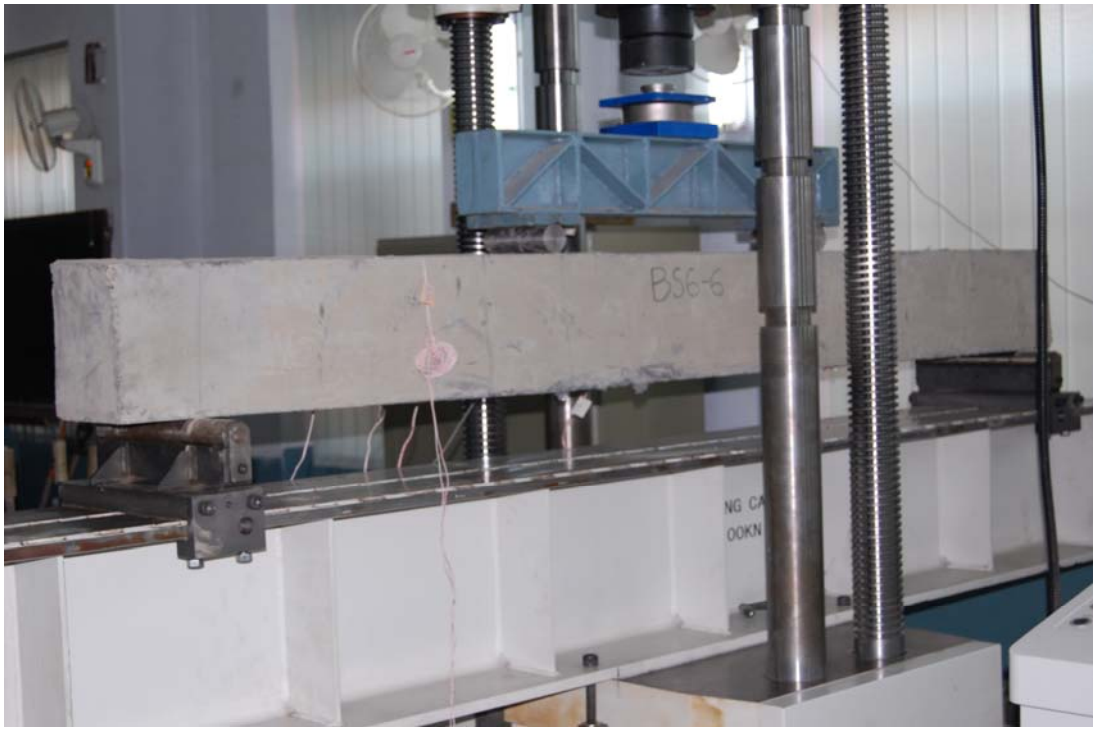


Fig 4.18 (a) - Cracking pattern BS 6-6


Fig 4.18 (b) - Cracking pattern BS 6-6

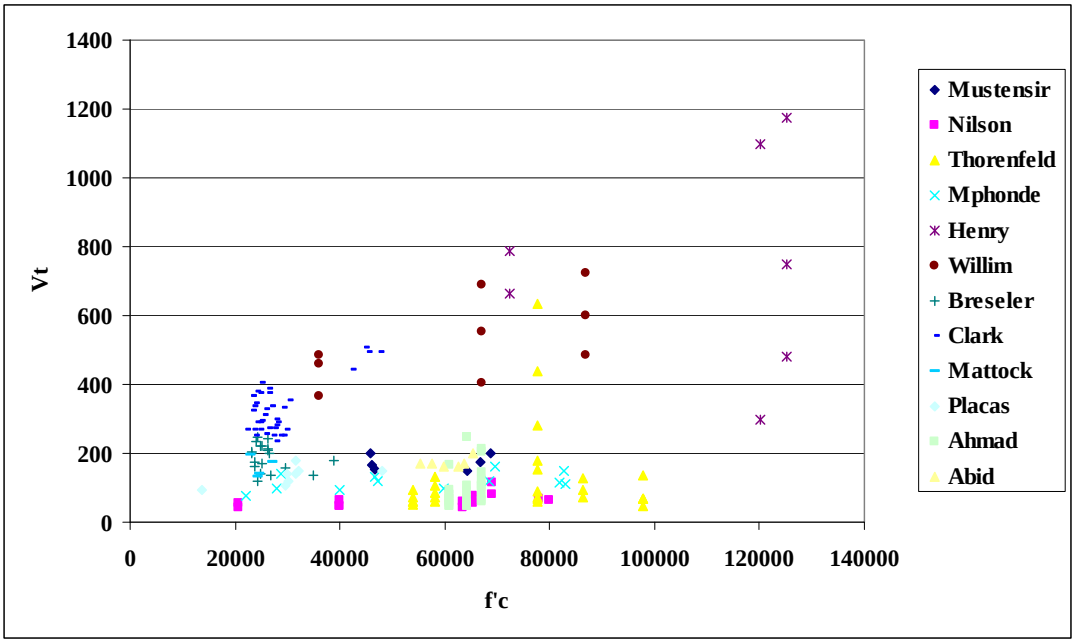


**Fig 5.1 -** $V_t$ **as a function of** $f_c^{/}$

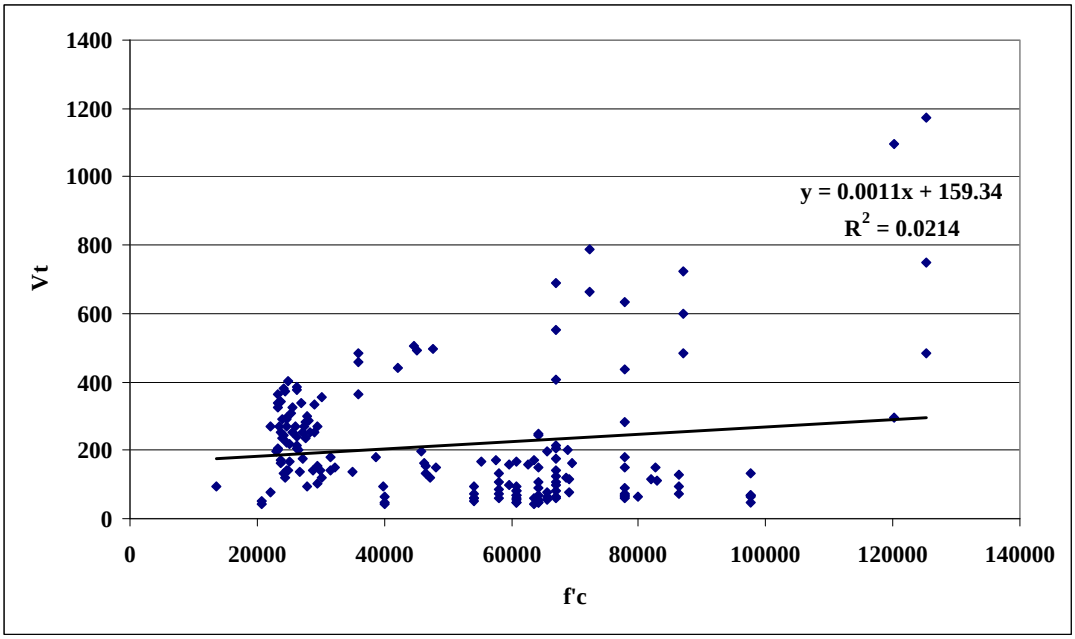


**Fig 5.2 -** $V_t$ **as a function of** $f_c^{/}$

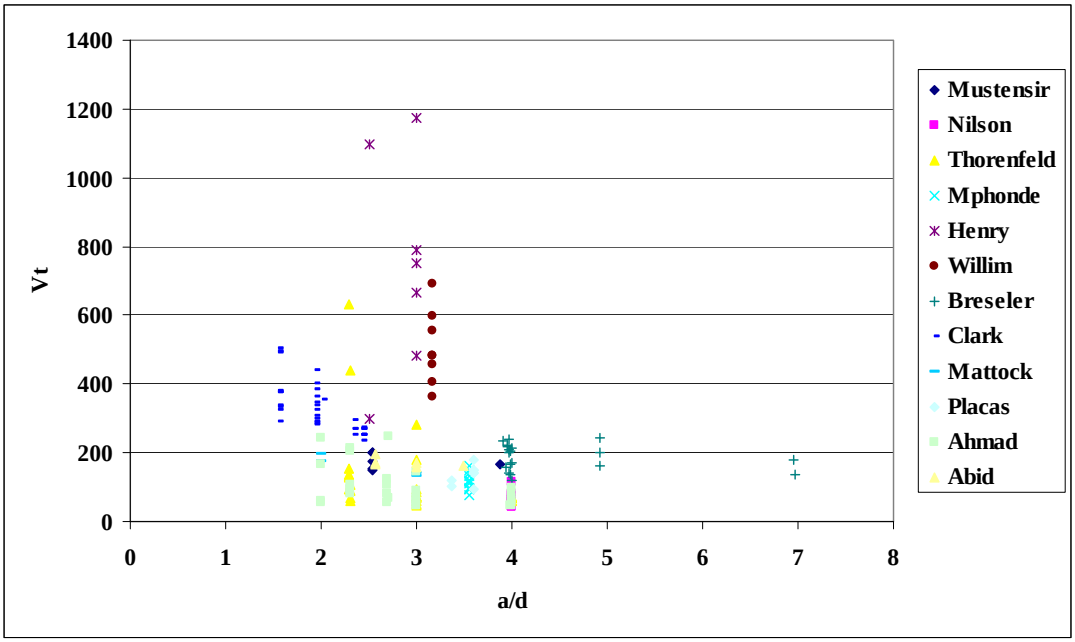


**Fig 5.3 -** $V_t$ **as a function of** $a/d$

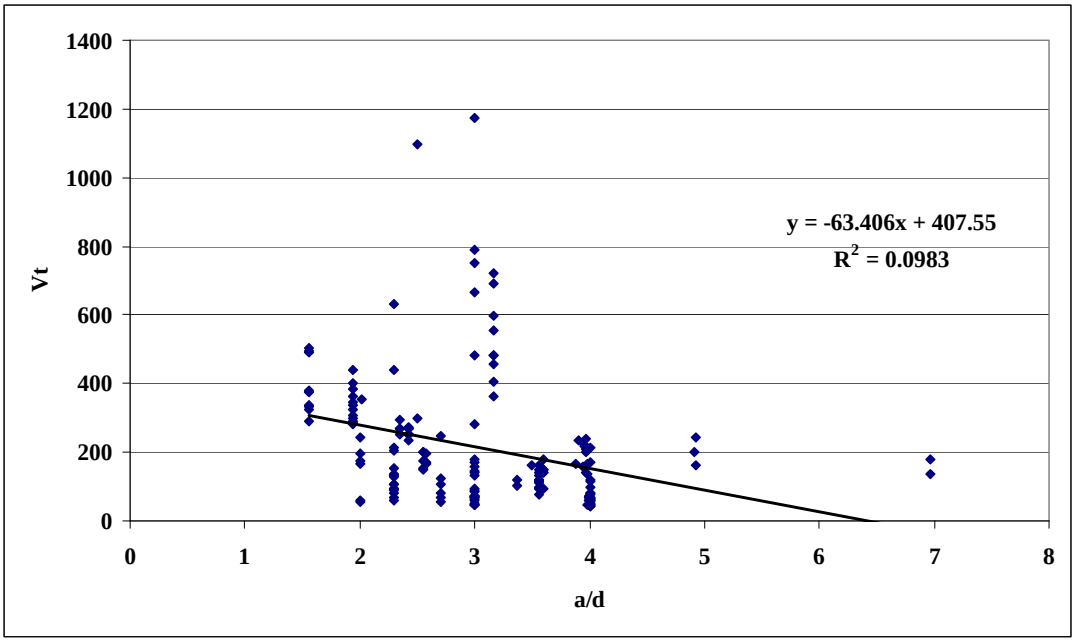


**Fig 5.4 -** $V_t$ **as a function of** $a/d$

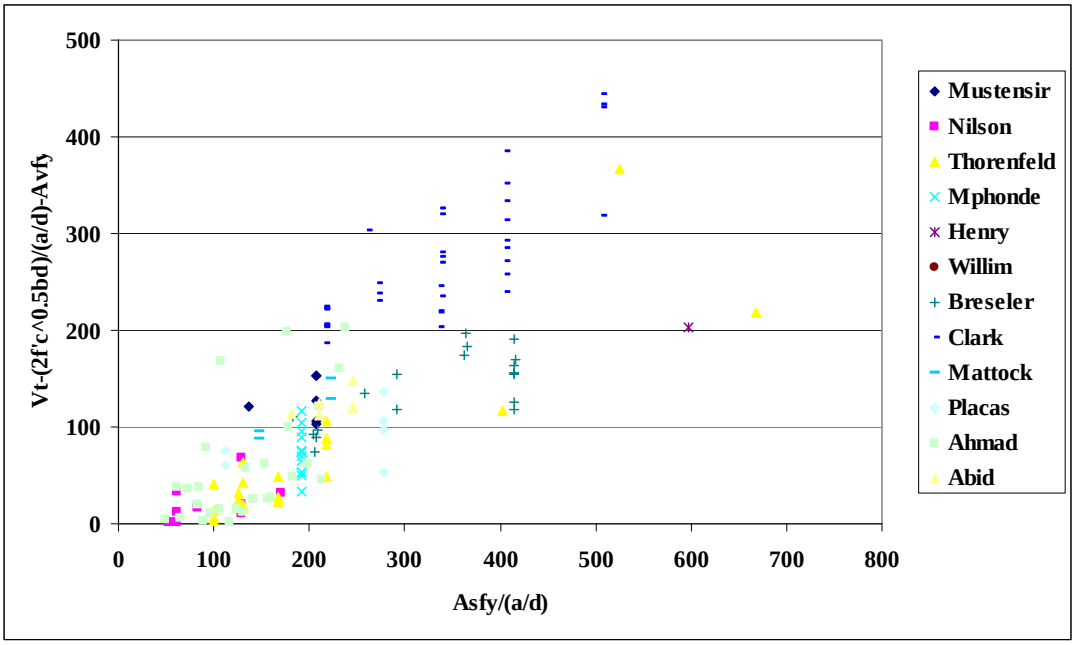


**Fig 5.5 -** $V_t - \dfrac{2\sqrt{f_c'}\,bd}{a/d} - A_V\, f_y$ **as a function of** $\dfrac{A_S\, f_y}{a/d}$

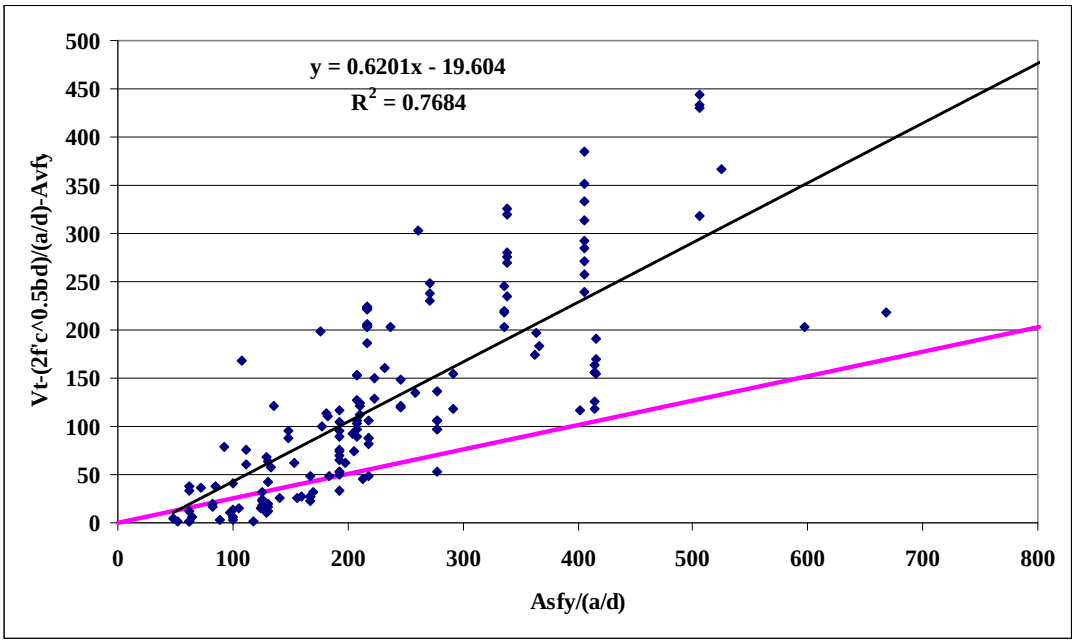


**Fig 5.6 -** $V_t - \dfrac{2\sqrt{f_c'}\,bd}{a/d} - A_V\,f_y$ **as a function of** $\dfrac{A_S\,f_y}{a/d}$

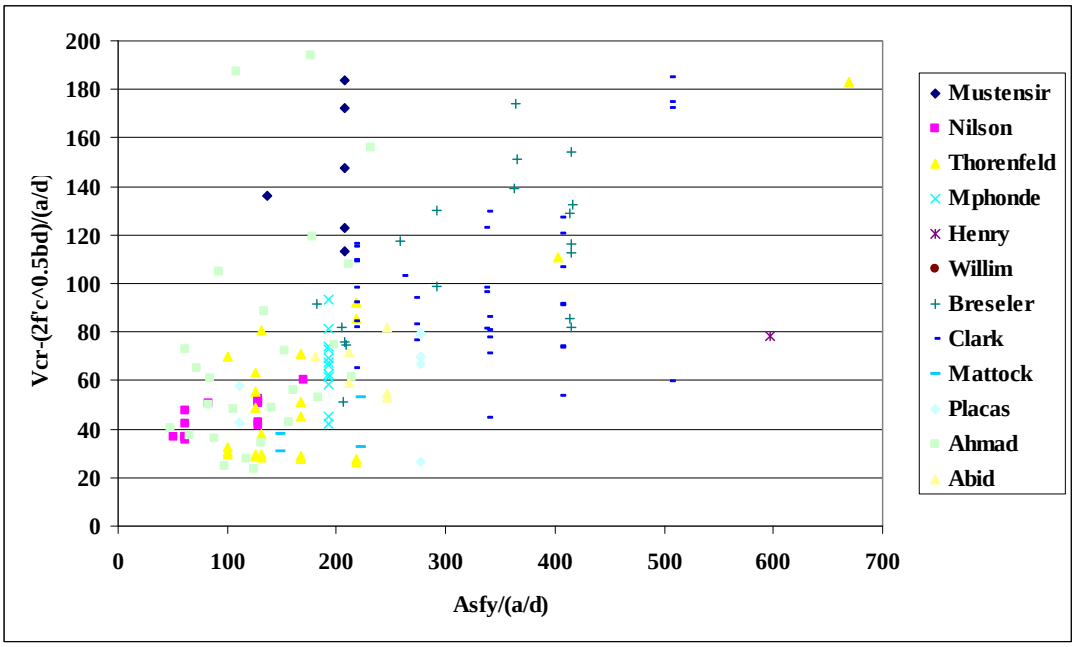


**Fig 5.7 -** $V_{cr} - \frac{2\sqrt{f_c'}bd}{a/d}$ **as a function of** $\frac{A_S f_y}{a/d}$

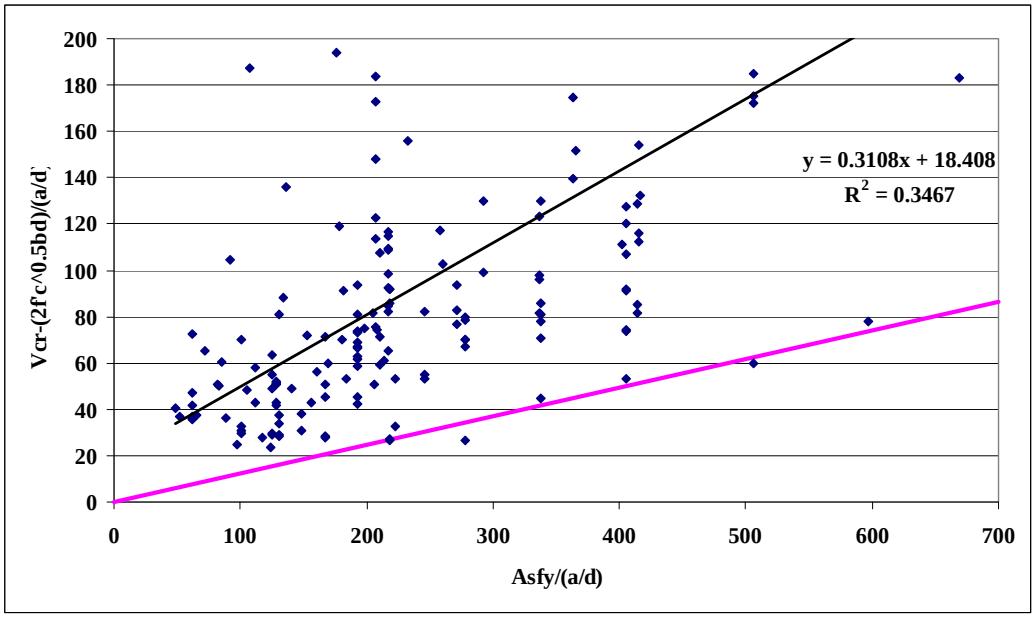


**Fig 5.8 -** $V_{cr} - \dfrac{2\sqrt{f_c'}bd}{a/d}$ **as a function of** $\dfrac{A_S f_y}{a/d}$